NASA CONTRACTOR REPORT

NASA CR-1316

c. 1

NASA CR-1316

TECH LIBRARY KAFB, NM
0069446

LOAN COPY: RETURN TO
AFWL (WLIL-2)
KIRTLAND AFB, N MEX

A THEORETICAL ANALYSIS OF THE FREE VIBRATION OF DISCRETELY STIFFENED CYLINDRICAL SHELLS WITH ARBITRARY END CONDITIONS

by D. M. Egle and K. E. Soder, Jr.

Prepared by
UNIVERSITY OF OKLAHOMA
Norman, Okla.
for Langley Research Center

RECEIVED
19 JUN 1969
Technical Library
AF Weapons Laboratory

NATIONAL AERONAUTICS AND SPACE ADMINISTRATION • WASHINGTON, D. C. • JUNE 1969

TECH LIBRARY KAFB, NM

0069446

NASA CR-1316

A THEORETICAL ANALYSIS OF THE FREE VIBRATION OF DISCRETELY STIFFENED CYLINDRICAL SHELLS WITH ARBITRARY END CONDITIONS

By D. M. Egle and K. E. Soder, Jr.

Distribution of this report is provided in the interest of information exchange. Responsibility for the contents resides in the author or organization that prepared it.

Prepared under Grant No. NGR 37-003-035 by
UNIVERSITY OF OKLAHOMA
Norman, Okla.

for Langley Research Center

NATIONAL AERONAUTICS AND SPACE ADMINISTRATION

For sale by the Clearinghouse for Federal Scientific and Technical Information
Springfield, Virginia 22151 – CFSTI price $3.00

ACKNOWLEDGEMENT

The work reported herein was sponsored by NASA grant NGR 37-003-035, under the technical direction of the Dynamic Loads Division, Langley Research Center, with Mr. John L. Sewall acting as grant monitor. The authors are indebted to the University of Oklahoma Computation Center for financial support of a portion of this project.

TABLE OF CONTENTS

	Page
LIST OF FIGURES	vi
LIST OF TABLES	viii
NOMENCLATURE	ix
INTRODUCTION	1
METHOD OF ANALYSIS	3
NUMERICAL RESULTS	27
CONCLUDING REMARKS	55
REFERENCES	57
APPENDIX I	62
APPENDIX II	65
APPENDIX III	72

LIST OF FIGURES

Figure		Page
1	Geometry of Discretely Stiffened Cylinder	6
2	Geometric Detail of Eccentric Stiffeners	9
3	Circumferential and Longitudinal Radial Mode Shapes (w) of a Cylinder	18
4	Theoretical and Experimental Frequencies of an Unstiffened Clamped-Free Cylindrical Shell	29
5	Theoretical and Experimental Frequencies of an Unstiffened Freely-Supported Cylindrical Shell	32
6	Minimum Frequency of a Cylindrical Shell as a Function of the Number of Stringers with the Total Stringer Area and Torsional Stiffness Constant	36
7	Theoretical and Experimental Frequencies of a Freely-Supported Cylindrical Shell with Thirteen Equally Spaced Rings	38
8	Theoretical Axial Modes of a Freely-Supported Cylinder with Thirteen Equally Spaced Symmetric Rings (N=2)	42
9	Theoretical Axial Modes of a Freely-Supported Cylinder with Thirteen Equally Spaced External Rings (N=2)	43
10	Theoretical Axial Modes of a Freely-Supported Cylinder with Thirteen Equally Spaced Symmetric Rings (N=10)	44
11	Theoretical Axial Modes of a Freely-Supported Cylinder with Thirteen Equally Spaced External Rings (N=10)	45
12	Theoretical and Experimental Frequencies of a Clamped-Free Cylindrical Shell with Three Rings and Sixteen Stringers	49
13	Theoretical Axial Modes of a Clamped-Free Cylinder with Three Rings and Sixteen Stringers (N=2)	52
14	Theoretical Axial Modes of a Clamped-Free Cylinder with Three Rings and Sixteen Stringers (N=9)	53

Figure		Page
15	Theoretical Axial Modes of a Clamped-Free Cylinder with Three Rings and Sixteen Stringers (N=11)	54

LIST OF TABLES

Table		Page
I	Shell Configurations used in Numerical Calculations	28
II	Theoretical and Experimental Frequencies of an Unstiffened Clamped-Free Cylinder	30
III	Theoretical and Experimental Frequencies of an Unstiffened Freely-Supported Cylinder	33
IV	Natural Frequencies of a Freely-Supported Cylindrical Shell with Four Internal Stringers	34
V	Theoretical Frequencies of a Freely-Supported Cylinder with Thirteen Equally Spaced Rings	39
VI	Natural Frequencies of a Cylinder with Seven External Rings	47
VII	Theoretical and Experimental Frequencies of a Clamped-Free Cylinder with Three Rings and Sixteen Stringers	50

NOMENCLATURE

a	length of cylindrical shell.
A_{rk}, $A_{s\ell}$	cross-sectional area of the kth ring, ℓ^{th} stringer.
D	isotropic plate flexural stiffness, $Et^3/12(1-\nu^2)$.
e	strains.
E_c	shell elastic modulus.
E_{rk}, $E_{s\ell}$	elastic modulus of the kth ring, ℓ^{th} stringer.
$(GJ)_{rk}$, $(GJ)_{s\ell}$	torsional stiffness of the kth ring, ℓ^{th} stringer.
i, j, k, l, m, n, P, Q	integers.
$I_{zzs\ell}$, I_{zzrk}	moment of inertia of the ℓth stringer, k^{th} ring cross-sectional area about an axis passing through the line of attachment and parallel to the z-axis. See Figure 2.
$I_{yzs\ell}$, I_{xzrk}	product of inertia of the ℓth stringer, k^{th} ring cross-sectional area about the yz, xz axes passing through the line of attachment. See Figure 2.
$I_{yys\ell}$, I_{xxrk}	moment of inertia of the ℓth stringer, k^{th} ring cross-sectional area about the y, x axis passing through the line of attachment. See Figure 2.
$I_{css\ell}$, I_{csrk}	cross stiffening parameters for the ℓth stringer, k^{th} ring. See Appendix I.
K	total number of rings.
L	total number of stringers.
m	axial wave number.
m^*	maximum number of terms used in the axial displacement series.
n	number of circumferential full waves.

n^*	maximum number of terms used in the circumferential displacement series.
R	radius of shell middle surface.
t	shell thickness
T	kinetic energy; $\ln\left(\frac{R+t/2}{R-t/2}\right)$
V	potential energy.
u, v, w	shell middle surface displacements in the x, θ, z directions.
$X_m(x)$	Bernoulli-Euler beam eigenfunctions.
$U_m(x), V_m(x), W_m(x)$	axial mode functions representing displacements in the x, θ, z directions.
$\bar{y}_{s\ell}, \bar{z}_{s\ell}$ $\bar{x}_{rk}, \bar{z}_{rk}$	coordinates of ℓth stringer, k^{th} ring centroidal axis referred to line of attachment. See Figure 2.
$\hat{y}_{s\ell}, \hat{z}_{s\ell}$ $\hat{x}_{s\ell}, \hat{z}_{s\ell}$	coordinates of ℓth stringer, k^{th} ring elastic axis referred to line of attachment. See Figure 2.
δ_{ij}	Kronecker delta function.
Δ	frequency parameter, $(1-\nu^2)\rho_c R^2\omega^2/E_c$.
ν	Poisson's ratio of shell material.
ρ_c	shell density.
$\rho_{rk}, \rho_{s\ell}$	density of kth ring, ℓ^{th} stringer.
ϕ_r, ϕ_s	angle of twist of a ring, stringer cross section about its elastic axis.
ω	circular frequency.
τ	time

Subscripts

c	refers to cylinder
k	refers to the kth ring
ℓ	refers to the ℓth stringer

r	refers to rings.
s	refers to stringers.

A comma before a subscript denotes partial differentation with respect to that subscript; e.g., $v_{,y}$ denotes $\partial v/\partial y$ and $w_{,xx}$ denotes $\partial^2 w/\partial x^2$.

INTRODUCTION

The vibration analysis of stiffened cylindrical shells has been and continues to be of considerable interest to structural analysts because of the wide spread use of this or similar type structures in air, space, and water craft. The degree of interest and the complexity of the problem are reflected in the number of publications in the literature devoted to this topic.

The investigative efforts may be divided into two broad classes: those which consider the stiffeners to be closely spaced and which average or "smear" the stiffening effects over the entire surface of the shell thus effectively replacing the stiffened shell by an orthotropic shell; and those which do not consider the stiffeners to be closely spaced and do not take advantage of the simplification of averaging the stiffener effects. References (1-15) apply the averaging technique to the analysis of stiffened shells while the discrete approach is used in references (16-47).

The more recent studies using the averaged stiffener approach (10-15) have been concerned with the effect of stiffener eccentricity and have included that effect explicitly. Of those investigations using the discrete approach, references (16-20) are concerned with stringer stiffened shells, references (21-40) deal with ring stiffened cylinders, and references (41-47) have considered both ring and stringer stiffeners.

The present effort may be considered an extension of the work in reference (46) and the theory and part of the numerical results are, in essence, the same as that of reference (47). In this report, an analysis

of the free vibrational characteristics of a thin uniform cylindrical shell with arbitrary end conditions and with an arbitrary number of ring and stringer stiffeners is developed. The stiffeners may be arbitrarily spaced and need not be identical but are assumed to be uniform along the stiffener axis. The analysis considers the effects of the flexure and extension of the shell; the flexure (about two perpendicular axes), extension, and torsion of the stiffeners, including the possibility of nonsymmetric stiffener cross sections. Stiffener flexural cross stiffening is also included in an approximate manner. The three translational shell inertia components and all six of the stiffener inertia components are considered. The problem is formulated by the energy method and the Rayleigh-Ritz technique is used to obtain an approximate solution.

Numerical results for several configurations of stiffened cylinders are presented and compared to existing theoretical and experimental frequencies. The stiffened shells considered include freely supported stringer-stiffened and ring-stiffened cylinders, a clamped-free ring and stringer-stiffened shell and a clamped-clamped ring stiffened shell.

METHOD OF ANALYSIS

The method of analysis utilized is the Rayleigh-Ritz energy technique. The general approach of the method is outlined in the following steps.

First, the expressions for the kinetic and potential energies are written for the cylinder, stringers, and rings. These six expressions are then used to give one expression for the total kinetic energy and one for the total potential energy of the stiffened cylinder, which are then expressed in terms of the displacement of the middle surface of the cylinder. Next, deflection shapes are assumed in the form of a finite series with undetermined coefficients, where each term satisfies the appropriate end conditions. These assumed displacement series are substituted into the energy expressions, and Hamilton's principle is used to develop a linear eigenvalue problem in the undetermined coefficients. This eigenvalue problem is solved, allowing the calculation of the desired natural frequencies and mode shapes.

Detailed Analysis

The energy expressions are written first in terms of the strain energy and then the strains are written in terms of the displacements of the middle surface of the shell to give the energy expressions as functions of the displacements. Only the strain energy due to the normal strain in the direction of the stiffener axis and shear strain due to twisting about the stiffener axis are considered for the stiffeners. The normal strain includes the effects due to extension of the stiffener and bending of the stiffener about two axes. The rotatory inertia of the shell is considered

negligible; however, the rotatory inertia is included in the stiffener kinetic energy terms.

Potential Energies

The strain displacement relations for a cylindrical shell with the coordinates shown in Figure 1 are given by Flügge (48) as

$$e_{xx} = u_{,x} - z\, w_{,xx}$$

$$e_{\theta\theta} = \frac{v_{,\theta}}{R} - \frac{z w_{,\theta\theta}}{R(R+z)} + \frac{w}{R+z} \qquad \text{(1a-c)}$$

$$e_{x\theta} = \frac{u_{,\theta}}{R+z} + \frac{R+z}{R} v_{,x} - \left(\frac{z}{R} + \frac{z}{R+z}\right) w_{,x\theta}$$

where a comma before the subscript indicates differentiation with respect to the subscript ($w_{,x\theta} = \frac{\partial^2 w}{\partial x \partial \theta}$). These relationships are referred to as Flügge's exact strain relations, and assume that normals to the middle surface remain normal after straining and that the displacements are small.

The strain energy or the potential energy of the shell is found by considering a small element in a thin shell. Since the shell is considered thin, it is assumed that the normal stress σ_{zz} is zero throughout the element and that the out of plane shear stresses are negligible ($\sigma_{xz} = \sigma_{\theta z} = 0$). Hooke's law for an isotropic material in a state of plane stress is

$$\sigma_{xx} = \frac{E}{1-\nu^2}(e_{xx} + \nu e_{\theta\theta})$$

$$\sigma_{\theta\theta} = \frac{E}{1-\nu^2}(e_{\theta\theta} + \nu e_{xx}) \qquad \text{(2a-c)}$$

$$\sigma_{x\theta} = \frac{E}{2(1+\nu)} e_{x\theta}$$

The increment change in strain energy per unit volume for the small element is

$$dV_{vol} = \sigma_{xx} de_{xx} + \sigma_{\theta\theta} de_{\theta\theta} + \sigma_{x\theta}\, de_{x\theta} \tag{3}$$

Substituting (2a-c) into (3) and integrating gives the strain energy per unit volume as

$$V_{Vol} = \frac{E}{(1-\nu^2)} \left[\frac{e_{xx}^2}{2} + \frac{e_{\theta\theta}^2}{2} + \nu e_{xx} e_{\theta\theta} + \frac{(1-\nu)}{4} e_{x\theta}^2 \right] \tag{4}$$

The total energy of the shell is then the integral over the volume of the shell

$$V_c = \int_{Vol} V_{Vol}\, d(Vol) \tag{5}$$

or

$$V_c = \frac{E_c}{2(1-\nu^2)} \int_{-t/2}^{t/2} \int_0^{2\pi} \int_0^a \left[e_{xx}^2 + e_{\theta\theta}^2 + 2\nu e_{xx} e_{\theta\theta} + \frac{1-\nu}{2} e_{x\theta}^2 \right] (R+z)\, dx d\theta dz \tag{6}$$

where d (Vol) =(R+z) $dx d\theta dz$, and E_c is Young's modulus of the cylinder. The strain energy of the cylinder is obtained as a function of the displacement of the middle surface by substituting (1a-c) into equation (6) and integrating over the shell thickness. The potential energy for the cylindrical shell may then be written as

$$\begin{aligned} V_c = \frac{6D}{t^2} \int_0^{2\pi} \int_0^a \Bigg[& R u_{,x}^2 + \frac{v_{,\theta}^2}{R} + w^2 \frac{T}{t} + \frac{2 v_{,\theta} w}{R} \\ & + 2\nu \left[u_{,x} v_{,\theta} + w u_{,x} \right] + \left(\frac{1-\nu}{2}\right) \Bigg\{ u_{,\theta}^2 \frac{T}{t} + \left(\frac{R^2 + \frac{t^2}{4}}{R} \right) \\ & v_{,x}^2 + 2 u_{,\theta} v_{,x} \Bigg\} \Bigg] dx d\theta + \frac{D}{2} \int_0^{2\pi} \int_0^a \Bigg[R w_{,xx}^2 - 2 u_{,x} w_{,xx} \\ & + \frac{12}{t^3} \left(T - \frac{t}{R} \right) (w_{,\theta\theta}^2 + 2 w_{,\theta\theta} w) + \frac{2\nu}{R} (w_{,xx} w_{,\theta\theta} - w_{,xx} v_{,\theta}) \end{aligned} \tag{7}$$

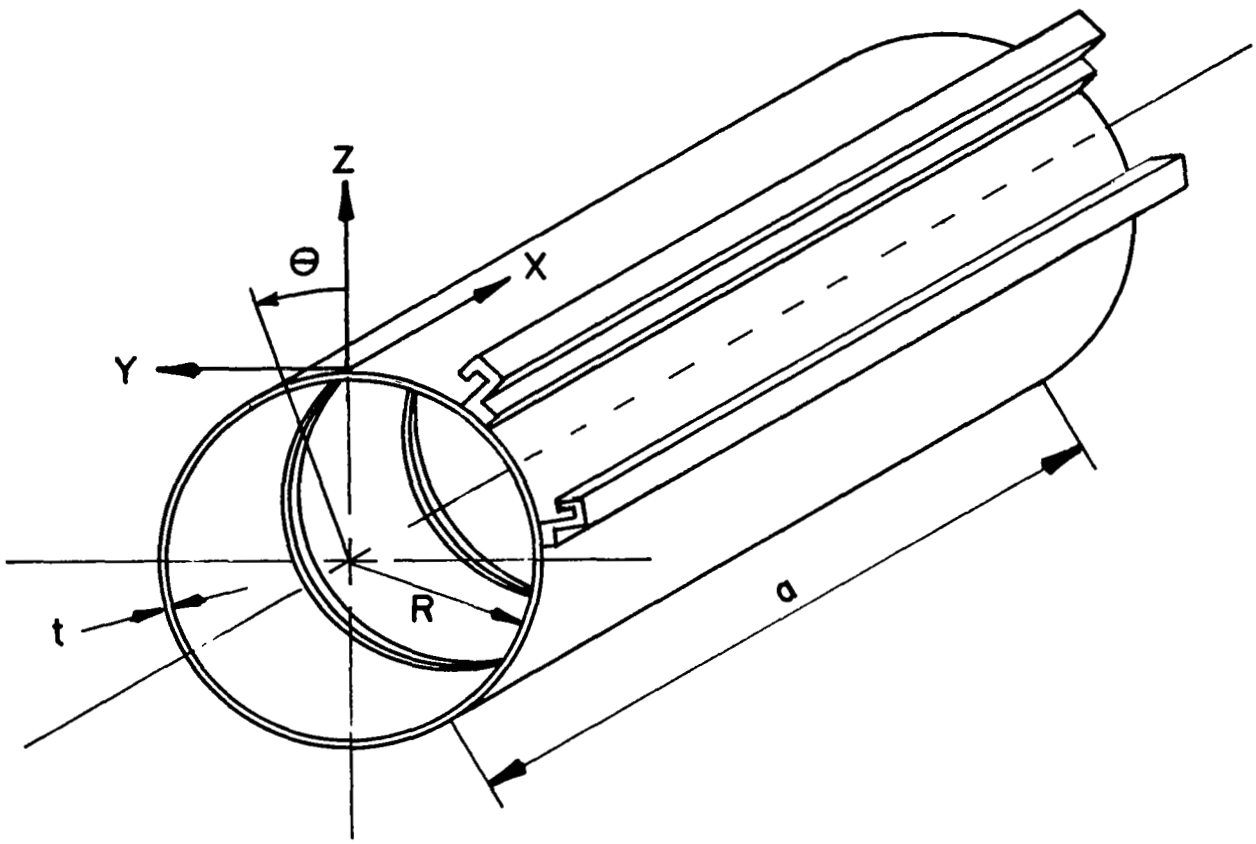

Figure 1. Geometry of Discretely Stiffened Cylinder

$$+ \left(\frac{1-\nu}{2}\right) \left\{ w_{,x\theta}^2 \left(R^2T - Rt + \frac{t^3}{4R}\right) \frac{12}{t^3} - \frac{6}{R} w_{,x\theta} v_{,x} \right. \qquad \text{(7 cont'd)}$$

$$\left. + \frac{24}{t^3} (RT - t) u_{,\theta} w_{,x\theta} \right\} \Bigg] dx d\theta$$

where $T = \ln \left(\frac{R + t/2}{R - t/2}\right)$

and $D = \frac{E_c t^3}{12(1-\nu^2)}$

This form of the shell potential energy can be shown to be equivalent to that developed by Miller (5) if the approximation

$$T \cong \frac{t}{R} + \frac{t^3}{12R^3}$$

is used in equation (7).

The potential energy expressions for the stringers and rings will be developed with the assumption that these stiffeners are uniform along their length and have an asymmetric cross section. Further, it is assumed that only normal strains in the direction of the stiffener axis and shearing strains due to twisting about the stiffener axis are important. It is also assumed that the cross sectional planes do not warp.

The elastic axis is chosen as a reference line for the stiffener since it remains undeformed in a state of pure torsion, and the deformations in this state may be described by a single variable, ϕ, the angular displacement of the cross section about the elastic axis. Since the elastic axis is chosen as the reference line, there is no coupling of the displacements of the elastic axis (u_E, v_E, w_E), which describe the flexural and extension in the bar, to the angular displacement (ϕ), which describes the torsion. Because of this uncoupling, the displacements of any point in a stringer (u_s, v_s, w_s) can be expressed as

$$u_s = u_E - y'v_{E,x} - z'w_{E,x}$$

$$v_s = v_E - z'\phi_s \tag{8a-c}$$

$$w_s = w_E + y'\phi_s$$

The coordinates are shown in the stringer detail of Figure 2.

The energy due to normal strain in the stringers is

$$V_{ext} = \sum_{\ell=1}^{L} \frac{E_{s\ell}}{2} \int_o^a \int_{A_{s\ell}} \left[e_{xx}^2\right]_{\theta=\theta_\ell} dA_{s\ell}dx \tag{9}$$

where $e_{xx} = u_{s,x}$ and the total number of stringers is L. The Young's modulus for the ℓth stringer (9) is $E_{s\ell}$ and θ_ℓ is its θ-coordinate.

The potential energy of the stringers in terms of the displacements of the elastic axis and the angular displacement of the cross section may be obtained by substituting equations (8a-c) into (9). It should be kept in mind, however, that the final energy expression must be related to the shell displacements at junction of the stringer and the shell. It is somewhat simpler algebraically if these compatibility relations are introduced into equations (8) before they are substituted into the energy expression (9).

The compatibility relations are quite simple if it can be assumed that the stiffener is integral with the shell at a single, common line (line of attachment). This assumption is more easily justified if the stringer is welded, riveted (closely spaced), or actually integral to the shell with the width of the junction (or the distance, perpendicular to the stiffener axis, over which the junction may be considered integral) is small compared to the wave length of vibration. The waves referred to are those perpendicular to the stiffener. However, there are methods of

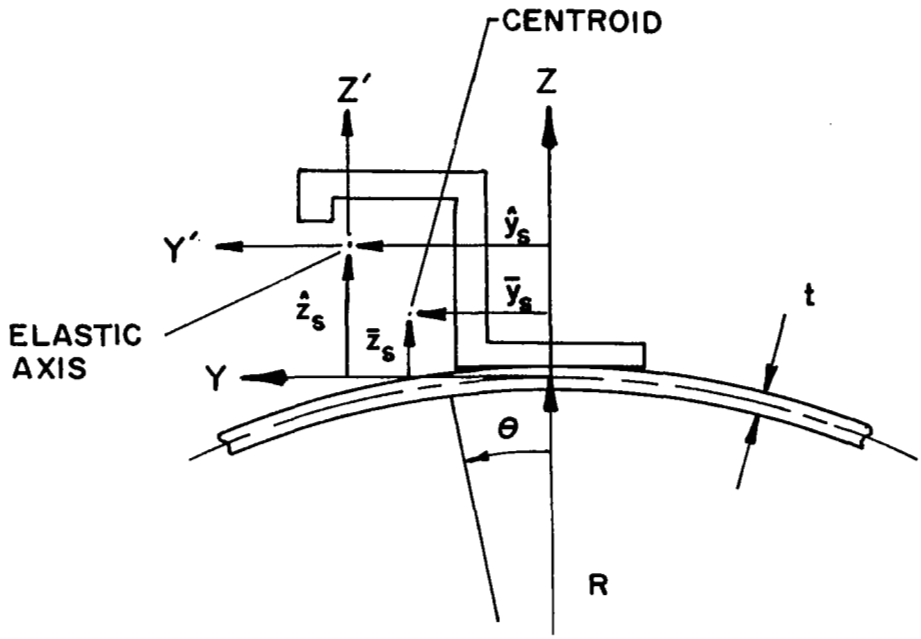

EXTERNAL STRINGER DETAIL

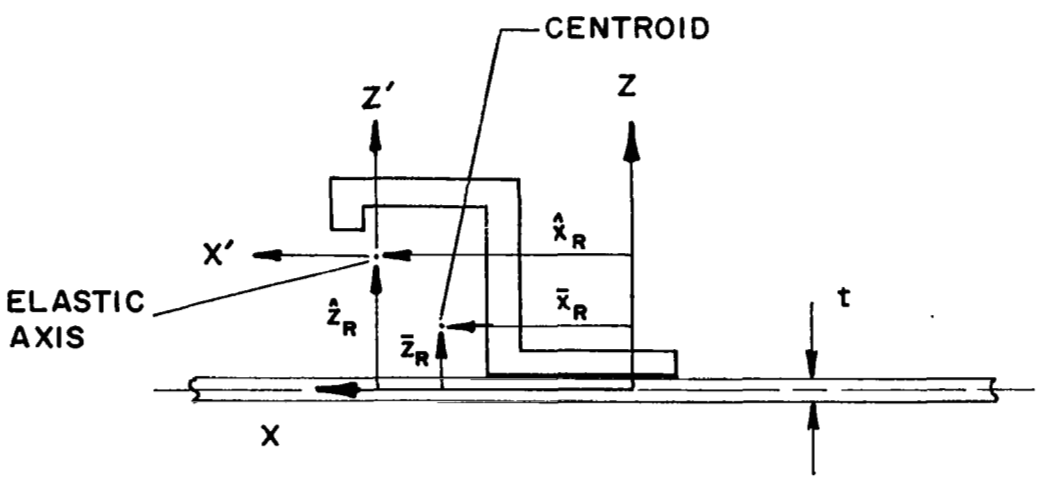

EXTERNAL RING DETAIL

Figure 2. Geometric Detail of Eccentric Stiffeners

attaching the stiffener to the shell which do not indicate a clear-cut line of attachment. As Ojalvo and Newman (19) have pointed out, an effective line of attachment must be assumed in these cases.

Assuming that the line of attachment has been determined, the displacement of this line (u_A, v_A, w_A) are first related to the elastic axis. This is done using the general equations (8a-c) and solving for the displacements of the elastic axis.

$$\begin{aligned} u_E &= u_A - \hat{y}_s v_{A,x} - \hat{z}_s w_{A,x} \\ v_E &= v_A - \hat{z}_s \phi_s \\ w_E &= w_A + \hat{y}_s \phi_s \end{aligned} \tag{10a-c}$$

If equations (10a-c) are substituted into (8a-c), there results

$$\begin{aligned} u_s &= u_A - y v_{A,x} - z w_{A,x} + (y\hat{z}_s - z\hat{y}_s)\, \phi_{s,x} \\ v_s &= v_A - z\phi_s \\ w_s &= w_A + y\phi_s \end{aligned} \tag{11a-c}$$

Compatibility between the shell and the stringer at the line of attachment requires

$$\begin{aligned} u_A &= u(x, \theta_\ell, \tau) \\ v_A &= v(x, \theta_\ell, \tau) \\ w_A &= w(x, \theta_\ell, \tau) \\ \phi_s &= (1/R)\, w_{,\theta}(x, \theta_\ell, \tau) \end{aligned} \tag{12a-d}$$

After substituting equations (11) into (9), carrying out the integration over the cross-sectional area of the stringer, and noting the compatibility relations, the stringer normal strain energy can be shown to be

$$
\begin{aligned}
V_{ext} = \sum_{\ell=1}^{L} \frac{E_{s\ell}}{2} \int_o^a \Big[& A_{s\ell} u_{,x}^2 - 2\bar{y}_{s\ell} A_{s\ell}\, u_{,x} v_{,xx} \\
& - 2\bar{z}_{s\ell} A_{s\ell}\, u_{,x} w_{,xx} + I_{zzs\ell} v_{,xx}^2 + 2I_{yzs\ell} v_{,xx} w_{,xx} \\
& + I_{yys\ell} w_{,xx}^2 \Big]_{\theta=\theta_\ell} dx + \frac{E_{s\ell}}{2} \int_o^a \Big[\frac{\Gamma_{s\ell}}{R^2} w_{,\theta xx}^2 \\
& + \frac{2A_{s\ell}}{R} (\bar{y}_{s\ell}\hat{z}_{s\ell} - \bar{z}_{s\ell}\hat{y}_{s\ell})\, u_{,x} w_{,\theta xx} - \frac{2}{R} (I_{zzs\ell}\hat{z}_{s\ell} \\
& - I_{yzs\ell}\hat{y}_{s\ell})\, v_{,xx} w_{,\theta xx} - \frac{2}{R} (I_{yzs\ell}\hat{z}_{s\ell} \\
& - I_{yys\ell}\hat{y}_{s\ell})\, w_{,xx} w_{,\theta xx} \Big]_{\theta=\theta_\ell} dx
\end{aligned}
\tag{13,a}
$$

where $\Gamma_{s\ell} = I_{zzs\ell}\hat{z}_{s\ell}^2 - 2I_{yzs\ell}\,\hat{z}_{s\ell}\,\hat{y}_{s\ell} + I_{yys\ell}\,\hat{y}_{s\ell}^2$

The terms in the first integral of equation (13,a) represent the extension, extension-flexure coupling (due to stringer eccentricity), and the flexure in the stringer. The terms in the second integral are the contributions of the twist in the stringer to the normal strain energy and the coupling between torsion and flexure and extension. As will be discussed later, numerical calculations for rectangular and wide flange section ring stiffeners with positive eccentricity indicate that the torsion and the torsion-flexure terms have very little effect. For this reason, the terms in the second integral of equation (13,a) will be neglected for this analysis.

If the stringer is not attached to the shell at a single common line, but is integral with the width of the stringer at the junction such that it cannot be considered small, the stiffness of the shell, perpendicular

to the stringer axis, will be increased at the stringer location. It is shown in Appendix I that this cross stiffening effect for the stringers may be approximated by

$$V_{cs} = \sum_{\ell=1}^{L} \frac{1}{2} E_{s\ell} I_{css\ell} \int_{o}^{a} (1/R^4)[w,^2_{\theta\theta}]_{\theta=\theta_\ell} dx \qquad (13,b)$$

where $I_{css\ell}$ is a cross stiffening parameter for the ℓth stringer defined in Appendix I.

The shear strain energy due to torsion of the stringers is taken in the form

$$V_{tor} = \sum_{\ell=1}^{L} \frac{(GJ)_{s\ell}}{2R^2} \int_{o}^{a} \left[w,^2_{x\theta}\right]_{\theta=\theta_\ell} dx \qquad (14)$$

where $(GJ)_{s\ell}$ is the torsional stiffness of the ℓth stringer. The total strain energy of the stringers (V_s) is equal to the sum of the extensional strain energy (V_{ext}), the strain energy due to the shear of torsion (V_{tor}) and the cross stiffening strain energy (V_{cs})

The strain energy of the rings may be developed in a manner similar to that used for the stringers. Using the elastic axis as a reference, the displacement at any point in a ring is

$$u_r = u_E - z'\phi_r$$

$$v_r = (1 + \frac{z'}{R_E}) v_E - \frac{z'}{R_E} w_{E,\theta} - \frac{x'}{R_E} u_{E,\theta} \qquad (15a\text{-}c)$$

$$w_r = w_E + x'\phi_r$$

where R_E is the radius of the elastic axis. The coordinates are shown in the ring detail of Figure 2.

The energy due to normal strain in the rings is

$$V_{ext} = \sum_{k=1}^{K} \frac{E_{rk}}{2} \int_{o}^{2\pi} \int_{A_{rk}} [\varepsilon_{\theta\theta}^2]_{x=x_k} \, dA_{rk} \, (R_E + z') \, d\theta \tag{16}$$

where $\varepsilon_{\theta\theta} = \frac{1}{R_E + z'} (v,_\theta + w)$ (17)

A considerable simplification in the analysis will result from assuming that the ring depth is small compared to the radius ($z'/R_E << 1$, and $R_E = R$). While this assumption is more restrictive than those used in the derivation of equation (7) for the shell potential energy, the increased accuracy gained by relaxing it seems to be greatly out of proportion to the increase in complexity in the analysis. McElman, reference (13), showed that, for the smeared stiffener analysis, the effects of this assumption on the natural frequencies are very small. Introducing this approximation into equations (15, 16, and 17) results in

$$\begin{aligned} u_r &= u_E - z'\phi_r \\ v_r &= v_E - \frac{z'}{R} w_{E,\theta} - \frac{x'}{R} u_{E,\theta} \\ w_r &= w_E + x'\phi_r \end{aligned} \tag{18a-c}$$

$$V_{ext} = \sum_{k=1}^{K} \frac{E_{rk}}{2} \int_{o}^{2\pi} \int_{A_{rk}} [\varepsilon_{\theta\theta}^2]_{x=x_k} \, dA_{rk} \, R d\theta \tag{19}$$

$$\varepsilon_{\theta\theta} = \frac{1}{R} (v,_\theta + w) \tag{20}$$

Using the technique described above for the stringers, the displacements at any point in the ring (u_r, v_r, w_r) may be related to the displacements at the line of attachment of the ring (u_A, v_A, w_A). Thus

$$\begin{aligned} u_r &= u_A - z\,\phi_r \\ v_r &= v_A - \frac{z}{R} w_{A,\theta} - \frac{x}{R} u_{A,\theta} + \frac{(\hat{z}_r\, x - \hat{x}_r\, z)}{R} \phi_{r,\theta} \end{aligned} \tag{21a-c}$$

$$w_r = w_A + x\,\phi_r \qquad \text{(21a-c Cont'd)}$$

The compatibility relations for the rings are

$$\begin{aligned} u_A &= u(x_k, \theta, \tau) \\ v_A &= v(x_k, \theta, \tau) \\ w_A &= w(x_k, \theta, \tau) \\ \phi_r &= w,_x (x_k, \theta, \tau) \end{aligned} \qquad \text{(22a-d)}$$

Combining equations (19, 20, 21 and 22) results in

$$\begin{aligned} V_{ext} = \sum_{k=1}^{K} \Bigg\{ \frac{E_{rk}}{2} \int_0^{2\pi} \Bigg[& \frac{A_{rk}}{R} v,_\theta^2 - \frac{2\bar{z}_{rk}A_{rk}}{R^2} v,_\theta w,_{\theta\theta} \\ & - \frac{2\bar{x}_{rk}A_{rk}}{R^2} v,_\theta u,_{\theta\theta} + \frac{I_{xxrk}}{R^3} w,_{\theta\theta}^2 + \frac{I_{zzrk}}{R^3} u,_{\theta\theta}^2 \\ & + 2\frac{I_{xzrk}}{R^3} u,_{\theta\theta} w,_{\theta\theta} + 2\frac{A_{rk}}{R} v,_\theta w - 2\frac{\bar{z}_{rk}A_{rk}}{R^2} w w,_{\theta\theta} \\ & - 2\frac{\bar{x}_{rk}A_{rk}}{R^2} w u,_{\theta\theta} + \frac{A_{rk}}{R} w^2 + 2\frac{\bar{x}_{rk}A_{rk}}{R} w,_x v,_\theta \\ & - 2\frac{I_{zzrk}}{R^2} u,_{\theta\theta} w,_x + 2\frac{\bar{x}_{rk}A_{rk}}{R} w\, w,_x + \frac{I_{zzrk}}{R} w,_x^2 \\ & - 2\frac{I_{xzrk}}{R^2} w,_x w,_{\theta\theta} \Bigg]_{x=x_k} d\theta + \frac{E_{rk}}{2} \int_0^{2\pi} \Bigg[\frac{\Gamma_{rk}}{R^3} w,_{x\theta\theta}^2 \\ & + \frac{2A}{R^2} (\hat{z}_{rk}\bar{x}_{rk} - \hat{x}_{rk}\bar{z}_{rk}) v,_\theta w,_{x\theta\theta} + \frac{2}{R^3} (\hat{z}_{rk}I_{xzrk} \\ & - \hat{x}_{rk}I_{xxrk}) w,_{\theta\theta} w,_{x\theta\theta} - \frac{2}{R^3} (\hat{z}_{rk}I_{zzrk} - \hat{x}_{rk}I_{xzrk}) u,_{\theta\theta} w,_{x\theta\theta} \\ & + \frac{2A_{rk}}{R^2} (\hat{z}_{rk}\bar{x}_{rk} - \hat{x}_{rk}\bar{z}_{rk}) w w,_{x\theta\theta} + \frac{2}{R^2} (\hat{z}_{rk}I_{zzrk} \\ & - \hat{x}_{rk}I_{xzrk}) w,_x w,_{x\theta\theta} \Bigg]_{x=x_k} d\theta \Bigg\} \end{aligned} \qquad \text{(23,a)}$$

where

As in the case of the stringers, the terms in the second integral of equation (23,a) will be neglected.

The strain energy due to flexural cross stiffening of the rings is shown in Appendix I to be approximated by

$$V_{cs} = \sum_{k=1}^{K} \frac{1}{2} E_{rk} I_{csrk} \int_{o}^{2\pi} [w,_{xx}]^2_{x=x_k} R d\theta \tag{23,b}$$

where I_{csrk} is the cross stiffening parameter of the kth ring defined in Appendix I.

The shear strain energy due to torsion in the rings is

$$V_{tor} = \sum_{k=1}^{K} \frac{(GJ)_{rk}}{2R} \int_{o}^{2\pi} [w,^2_{x\theta}]_{x=x_k} d\theta \tag{24}$$

where $(GJ)_{rk}$ is the torsional stiffness of the kth ring. The total strain energy of the rings (V_r) is equal to the sum of the extensional strain energy (V_{ext}), the strain energy due to torsion (V_{tor}) and the cross stiffening strain energy, (V_{cs}).

Kinetic Energies

Neglecting the rotatory inertia, the kinetic energy of the shell may be written as

$$T_c = \frac{1}{2} \int_{o}^{2\pi} \int_{o}^{a} \rho_c \, t \, (\dot{u}^2 + \dot{v}^2 + \dot{w}^2) \, dx \, R d\theta \tag{25}$$

The kinetic energy of the stringers is

$$T_s = \frac{1}{2} \sum_{\ell=1}^{L} \rho_{s\ell} \int_{o}^{a} \int_{A_{s\ell}} [\dot{u}_s^2 + \dot{v}_s^2 + \dot{w}_s^2] \, dA_{s\ell} \, dx \tag{26}$$

where the dot over a variable indicates the time derivative.

Combining equations (11, 12, and 26) will give the kinetic energy of the stringers in terms of the displacement of the center surface of the shell.

$$
\begin{aligned}
T_s = \frac{1}{2} \sum_{\ell=1}^{L} \rho_{s\ell} \int_o^a \Big[& A_{s\ell} \, (\dot{u}^2 - 2\bar{y}_{s\ell} \, \dot{u} \, \dot{v}_{,x} - 2\bar{z}_{s\ell} \, \dot{u} \, \dot{w}_{,x} \\
& + \dot{v}^2 - (2/R) \, \bar{z}_{s\ell} \, \dot{v} \, \dot{w}_{,\theta} + \dot{w}^2 + (2/R) \, \bar{y}_{s\ell} \, \dot{w} \, \dot{w}_{,\theta}) \\
& + I_{zzs\ell} \, [\dot{v}_{,x}^2 + (1/R^2) \, \dot{w}_{,\theta}^2] + 2I_{yzs\ell} \, \dot{v}_{,x} \, \dot{w}_{,x} \\
& + I_{yys\ell} \, [\dot{w}_{,x}^2 + (1/R^2) \, \dot{w}_{,\theta}^2] \Big]_{\theta=\theta_\ell} dx
\end{aligned}
\tag{27}
$$

The terms in the stringer kinetic energy involving twisting ($\dot{w}_{,x\theta}^2$), twisting-translation coupling ($\dot{u} \, \dot{w}_{,x\theta}$) and twisting-rotation coupling ($\dot{v}_{,x} \, \dot{w}_{,x\theta}$ and $\dot{w}_{,x} \, \dot{w}_{,x\theta}$) have been omitted for consistency with the stringer potential energy.

The kinetic energy of the rings is

$$
T_R = \frac{1}{2} \sum_{k=1}^{K} \rho_{rk} \int_o^{2\pi} \int_{A_{rk}} [\dot{u}_r^2 + \dot{v}_r^2 + \dot{w}_r^2] \, dA_{rk} \, R d\theta \tag{28}
$$

Combining equations (21, 22, and 28) results in

$$
\begin{aligned}
T_R = \frac{1}{2} \sum_{k=1}^{K} \rho_{rk} \int_o^{2\pi} \Big[& A_{rk} \, [\dot{u}^2 - 2\bar{z}_{rk} \, \dot{u} \, \dot{w}_{,x} + \dot{w}^2 \\
& + 2\bar{x}_{rk} \, \dot{w} \, \dot{w}_{,x} + \dot{v}^2 - (2/R) \, \bar{z}_{rk} \, \dot{v} \, \dot{w}_{,\theta} - (2/R) \, \bar{x}_{rk} \, \dot{v} \, \dot{u}_{,\theta}] \\
& + I_{xxrk} \, [\dot{w}_{,x}^2 + (1/R^2) \, \dot{w}_{,\theta}^2] + (2/R^2) \, I_{xzrk} \, \dot{w}_{,\theta} \, \dot{u}_{,\theta} \\
& + I_{zzrk} \, [\dot{w}_{,x}^2 + (1/R^2) \, \dot{u}_{,\theta}^2] \Big]_{x=x_k} R d\theta
\end{aligned}
\tag{29}
$$

where the twisting, twisting-extension and twisting-rotation terms have been omitted for consistency.

Displacement Functions

The displacements of the middle surface of the cylinder (u,v,w) are assumed to be

$$u = \sum_m \sum_n (\bar{u}_{mn} \cos n\theta + \bar{u}'_{mn} \sin n\theta)\, U_m(x) \sin \omega\tau$$

$$v = \sum_m \sum_n (\bar{v}_{mn} \sin n\theta - \bar{v}'_{mn} \cos n\theta)\, V_m(x) \sin \omega\tau \qquad (30a\text{-}c)$$

$$w = \sum_m \sum_n (\bar{w}_{mn} \cos n\theta + \bar{w}'_{mn} \sin n\theta)\, W_m(x) \sin \omega\tau$$

where $U_m(x)$, $V_m(x)$, $W_m(x)$ are axial mode functions which are chosen to satisfy the end conditions. These functions are extended versions of those assumed in reference (17). Figure 3 identified a few of the terms in equation (30c) for simply-supported and clamped-free end conditions.

The unprimed coefficients ($\bar{u}_{mn}$, $\bar{v}_{mn}$, $\bar{w}_{mn}$) are associated with the symmetric circumferential modes, referring to those modes having normal displacements (w) which are symmetric with respect to the x-z plane. Similarly, the primed coefficients (u'_{mn}, v'_{mn}, w'_{mn}) are associated with the antisymmetric circumferential modes.

Axial Mode Functions

The axial mode functions $U_m(x)$, $V_m(x)$, and $W_m(x)$ should be selected to satisfy the end conditions of the particular stiffened shell under investigation. However, as Meirovitch (49) has indicated, the Rayleigh-Ritz technique does not require that the assumed displacement functions satisfy the force or moment end conditions, only those involving kinematic quantities (displacements or slope). The following sets of axial mode functions have been successfully implemented in this analysis.

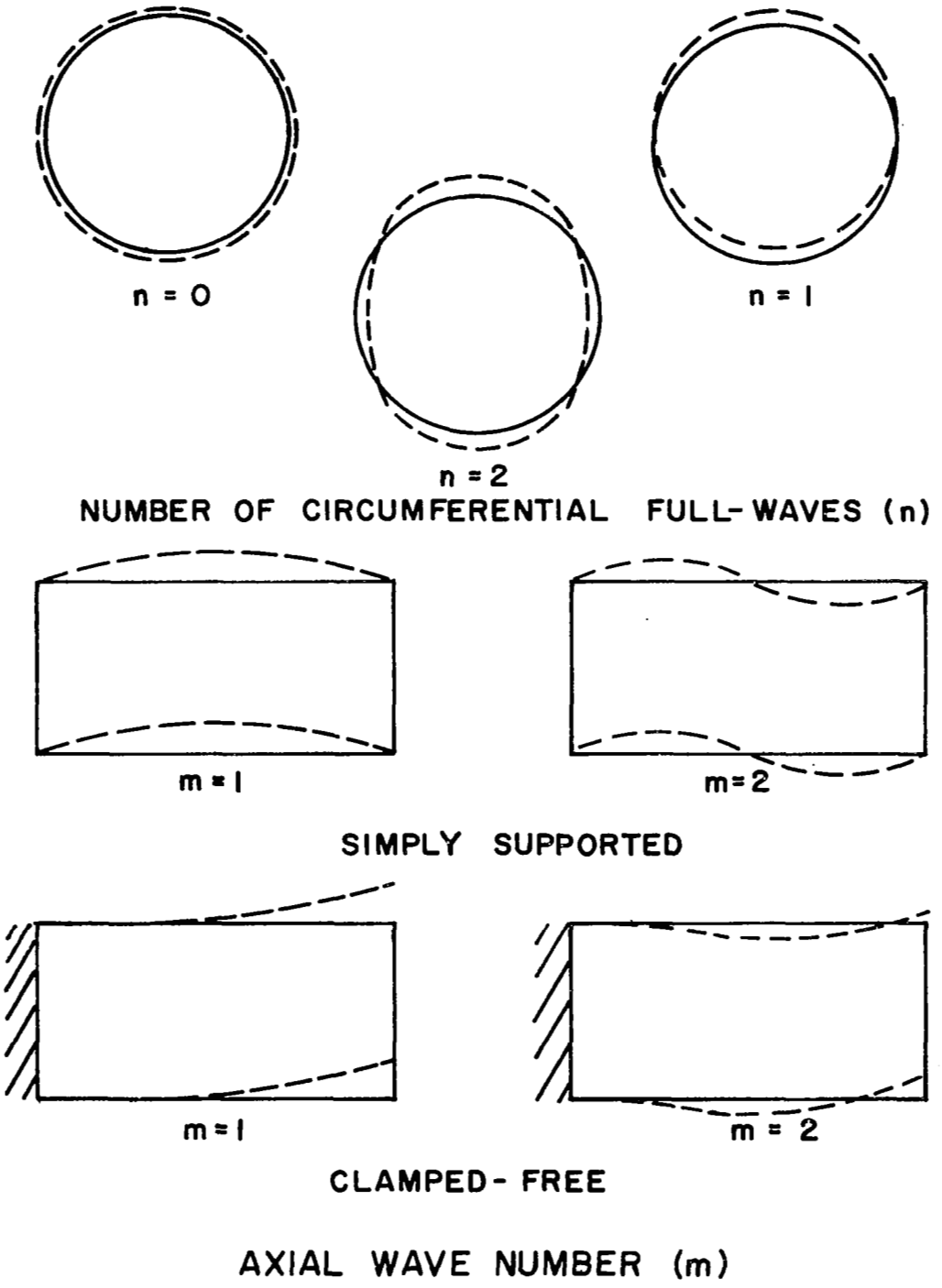

Figure 3. Circumferential and Longitudinal Radial Mode Shapes (w) of a Cylinder

Both ends simply supported without axial constraint (freely supported):

$$U_m(x) = \sqrt{2}\cos m\pi x/a$$

$$V_m(x) = \sqrt{2}\sin m\pi x/a \qquad (31a\text{-}c)$$

$$W_m(x) = \sqrt{2}\sin m\pi x/a$$

x = 0 clamped, x = a free:

$$U_m(x) = \frac{d\,X_m(x)}{d\,x}$$

$$V_m(x) = X_m(x) \qquad (32a\text{-}c)$$

$$W_m(x) = X_m(x)$$

where $X_m(x)$ are the Bernoulli-Euler clamped-free beam eigenfunctions

Both ends clamped: (see reference 50)

$$U_m(x) = \sin m\pi x/a$$

$$V_m(x) = \sin m\pi x/a \qquad (33a\text{-}c)$$

$$W_m(x) = \cos(m-1)\pi x/a - \cos(m+1)\pi x/a$$

Both ends simply supported with axial constraint:

$$U_m(x) = \sqrt{2}\sin m\pi x/a$$

$$V_m(x) = \sqrt{2}\sin m\pi x/a \qquad (34a\text{-}c)$$

$$W_m(x) = \sqrt{2}\sin m\pi x/a$$

The following sets of axial mode functions have not been implemented but may be useful for other end conditions.

Both ends free:

$$U_m(x) = \cos m\pi x/a$$

$$V_m(x) = \cos m\pi x/a$$

$$W_m(x) = \cos m\pi x/a$$

Note that the m=0 term should be included in this case to account for the rigid body modes.

x = 0 simply supported with axial constraint, x = a free:

$$U_m(x) = \sin (2m-1)\pi x/2a$$

$$V_m(x) = \sin (2m-1)\pi x/2a$$

$$W_m(x) = \sin (2m-1)\pi x/2a$$

Frequency Equation

The equations of motion for free vibration may be derived from Hamilton's principle

$$\delta \int_{\tau_1}^{\tau_2} (T - V)\, d\tau = 0 \tag{35}$$

where T and V are the total kinetic and potential energy of the shell, rings, and stringers given by

$$\begin{aligned} T &= T_c + T_r + T_s \\ V &= V_c + V_r + V_s \end{aligned} \tag{36a-b}$$

Combining equations (30, 35, and 36) results in the following equations linear in $\bar{u}_{mn}$, $\bar{v}_{mn}$, $\bar{w}_{mn}$, $\bar{u}'_{mn}$, $\bar{v}'_{mn}$, and $\bar{w}'_{mn}$

$$\sum_m \sum_n \Big[A_{ijmn}\bar{u}_{mn} + D_{ijmn}\bar{v}_{mn} + E_{ijmn}\bar{w}_{mn} + G_{ijmn}\bar{u}'_{mn} + GG_{ijmn}\bar{v}'_{mn}$$

$$+ H_{ijmn}\bar{w}'_{mn} - \Delta \Big[N_{ijmn}\bar{u}_{mn} + NN_{ijmn}\bar{v}_{mn} + P_{ijmn}\bar{w}_{mn}$$

$$+ T_{ijmn}\bar{u}'_{mn} + TT_{ijmn}\bar{v}'_{mn} + U_{ijmn}\bar{w}'_{mn} \Big] \Big] = 0$$

$$\sum_m \sum_n \Big[D_{mnij}\bar{u}_{mn} + B_{ijmn}\bar{v}_{mn} + F_{ijmn}\bar{w}_{mn} + FF_{ijmn}\bar{u}'_{mn}$$

$$+ EE_{ijmn}\bar{v}'_{mn} + DD_{ijmn}\bar{w}'_{mn} - \Delta \Big[NN_{mnij}\bar{u}_{mn} + Q_{ijmn}\bar{v}_{mn}$$

$$+ R_{ijmn}\bar{w}_{mn} + RR_{ijmn}\bar{u}'_{mn} + V_{ijmn}\bar{v}'_{mn} + W_{ijmn}\bar{w}'_{mn} \Big] \Big] = 0 \qquad (37a\text{-}d)$$

$$\sum_m \sum_n \Big[E_{mnij}\bar{u}_{mn} + F_{mnij}v_{mn} + C_{ijmn}\bar{w}_{mn} + HH_{ijmn}\bar{u}'_{mn}$$

$$+ MM_{ijmn}\bar{v}'_{mn} + M_{ijmn}\bar{w}'_{mn} - \Delta \Big[P_{mnij}\bar{u}_{mn} + R_{mnij}\bar{v}_{mn}$$

$$+ S_{ijmn}\bar{w}_{mn} + UU_{ijmn}\bar{u}'_{mn} + X_{ijmn}\bar{v}'_{mn} + Y_{ijmn}\bar{w}'_{mn} \Big] \Big] = 0$$

$$\sum_m \sum_n \Big[G_{mnij}\bar{u}_{mn} + FF_{mnij}\bar{v}_{mn} + HH_{mnij}\bar{w}_{mn} + A'_{ijmn}\bar{u}'_{mn}$$

$$+ D'_{ijmn}\bar{v}'_{mn} + E'_{ijmn}\bar{w}'_{mn} - \Delta \Big[T_{mnij}\bar{u}_{mn} + RR_{mnij}\bar{v}_{mn}$$

$$+ UU_{mnij}\bar{w}_{mn} + N'_{ijmn}\bar{u}'_{mn} + NN'_{ijmn}v'_{mn} + P'_{ijmn}\bar{w}'_{mn} \Big] \Big] = 0$$

$$\sum_m \sum_n \Big[GG_{mnij}\bar{u}_{mn} + EE_{mnij}\bar{v}_{mn} + MM_{mnij}\bar{w}_{mn} + D'_{mnij}\bar{u}'_{mn}$$

$$+ B'_{ijmn}\bar{v}'_{mn} + F'_{ijmn}\bar{w}'_{mn} - \Delta \Big[TT_{mnij}\bar{u}_{mn} + V_{mnij}\bar{v}_{mn}$$

$$+ X_{mnij}\bar{w}_{mn} + NN'_{mnij}\bar{u}'_{mn} + Q'_{ijmn}\bar{v}'_{mn} + R'_{ijmn}\bar{w}'_{mn} \Big] \Big] = 0$$

(37e-f)

$$\sum_m \sum_n \Big[H_{mnij}\bar{u}_{mn} + DD_{mnij}\bar{v}_{mn} + M_{mnij}\bar{w}_{mn} + E'_{mnij}\bar{u}'_{mn}$$

$$+ F'_{mnij}\bar{v}'_{mn} + C'_{ijmn}\bar{w}'_{mn} - \Delta \Big[U_{mnij}\bar{u}_{mn} + W_{mnij}\bar{v}_{mn}$$

$$+ Y_{mnij}\bar{w}_{mn} + P'_{mnij}\bar{u}'_{mn} + R'_{mnij}\bar{v}'_{mn} + S'_{ijmn}\bar{w}'_{mn} \Big] \Big] = 0$$

where $\Delta = (1-\nu^2)\ \rho_c\ R^2\omega^2/E_c$ is the frequency parameter. The coefficients in equations (37a-f)are presented in Appendix II.

Equations (37a-f) may also be written in matrix form, with the aid of the work of Egle and Sewall (46), as

$$\left[\begin{bmatrix} A & D & E & G & GG & H \\ D^T & B & F & FF & EE & DD \\ E^T & F^T & C & HH & MM & M \\ G^T & FF^T & HH^T & A' & D' & E' \\ GG^T & EE^T & MM^T & D'^T & B' & F' \\ H^T & DD^T & M^T & E'^T & F'^T & C' \end{bmatrix} - \Delta \begin{bmatrix} N & NN & P & T & TT & U \\ NN^T & Q & R & RR & V & W \\ P^T & R^T & S & UU & X & Y \\ T^T & RR^T & UU^T & N' & NN' & P' \\ TT^T & V^T & X^T & NN'^T & Q' & R' \\ U^T & W^T & Y^T & P'^T & R'^T & S' \end{bmatrix}\right] \begin{Bmatrix} \bar{\bar{u}} \\ \bar{\bar{v}} \\ \bar{\bar{w}} \\ \bar{\bar{u}}' \\ \bar{\bar{v}}' \\ \bar{\bar{w}}' \end{Bmatrix} = 0 \quad (38)$$

where the superscript T indicates the submatrix has been transposed. The

terms in equations (37a-f) have been redefined in order to write them in the matrix form of equation (38). The terms $\bar{\bar{u}}$, $\bar{\bar{v}}$, etc. are column vectors whose components are

$$\bar{\bar{u}}_P = \bar{u}_{mn}$$

$$\bar{\bar{v}}_P = \bar{v}_{mn}$$

$$\begin{matrix} \cdot & \cdot \\ \cdot & \cdot \\ \cdot & \cdot \end{matrix}$$

$$\bar{\bar{w}}'_P = \bar{w}'_{mn}$$

and n and m are related to P by

$$m = P - \left(\frac{P-1}{m^*}\right)_T m^*$$

$$n = 1 + \left(\frac{P-1}{m^*}\right)_T \qquad (39a\text{-}b)$$

where m^* is the maximum value of m, n^* is the maximum value of n, and the symbol $(\ )_T$ represents the operation of integer truncation, for example $(8/3)_T = 2$. Likewise, the coefficients A_{QP}, D_{QP}, etc. in the matrix are related to those in equations (37a-f) by

$$A_{QP} = A_{ijmn}$$

$$D_{QP} = D_{ijmn}$$

$$\begin{matrix} \cdot & \cdot \\ \cdot & \cdot \\ \cdot & \cdot \end{matrix}$$

$$S'_{QP} = S'_{ijmn}$$

where n and m are related to P by equations (39a-b), while i and j are related to Q by

$$j = Q - \left(\frac{Q-1}{m^*}\right)_T m^*$$

$$j = 1 + \left(\frac{Q-1}{m^*}\right)_T \qquad (40a\text{-}b)$$

An example of this calculation for P = 10, Q = 16, and m* = 4, gives i = 6, j = 4, m = 2, and n = 3, then $A_{10,16} = A_{6,4,2,3}$.

The solution of equation (38) is a linear eigenvalue problem whose size is (6m*n*) by (6m*n*). The first matrix in equation (38), which contains A, B, C, etc., will be referred to as the stiffness matrix, and the second matrix as the mass matrix.

Equations (37a-f and 38) will simplify if it is assumed that the stringers are distributed symmetrically with respect to the x-z plane. This means that for every stringer at $\theta=\theta_\ell$ there is a mirror image stringer at $\theta=-\theta_\ell$. Thus, if a stringer at $\theta=\theta_\ell$ has a $\bar{y}_{s\ell}$ or a $I_{yzs\ell}$ that is not zero, the corresponding stringer at $\theta=\theta_\ell$ must be identical with the exception that $\bar{y}_{s\ell}$ and $I_{yzs\ell}$ must be the negative of that of the stringer at $\theta=\theta_\ell$. Stringers located at $\theta=0$, π must have $\bar{y}_{s\ell} = 0$, $I_{yzs\ell} = 0$ to satisfy this symmetry. The terms in equation (38) which couple the symmetric and antisymmetric circumferential modes (G, GG, H, FF, EE, DD, HH, MM, and M in the stiffness matrix; and T, TT, U, RR, V, W, UU, X, and Y in the mass matrix) are identically zero for this stringer distribution. For example,

$$GG_{ijmn} = I_{V_m''U_i''}R^2 \sum_{\ell=1}^{L/2} S_{s\ell}\,[\bar{y}_{s\ell} \cos(n\theta_\ell) \cos(j\theta_\ell) - \bar{y}_{s\ell} \cos(-n\theta_\ell) \cos(-j\theta_\ell)] = 0$$

and

$$G_{ijmn} = I_{U'_m U'_i} R^2 \sum_{\ell=1}^{L/2} S_{s\ell} \left[\sin(n\theta_\ell) \cos(j\theta_\ell) + \sin(-n\theta_\ell) \cos(-j\theta_\ell)\right] = 0$$

For this special stringer distribution, equations (38) reduce to two uncoupled sets of equations. The existence of "double resonances" is implied from the fact that these two sets of equations are not necessarily equal. This phenomenon was discussed in reference (46).

Computer Program

Equations (38) were programmed for solution on an IBM 360/40 digital computer. The available memory (120 K bytes) limited the maximum number of terms m*n*) in the displacement series (30) to seven or a (42x42) eigenvalue problem. It was soon discovered that seven terms in the displacement series were insufficient for accurate results on some ring stiffened shells. Thus, in order to increase the maximum number of terms in the assumed displacement series, the mirror image stringer distribution described previously was assumed. This allows the solution for the symmetric and antisymmetric modes to be calculated independently. The equations governing the symmetric circumferential modes are

$$\left[\begin{bmatrix} A & D & E \\ D^T & B & F \\ E^T & F^T & C \end{bmatrix} - \Delta \begin{bmatrix} N & NN & T \\ NN^T & Q & R \\ P^T & R^T & S \end{bmatrix}\right] \begin{Bmatrix} \bar{\bar{u}} \\ \bar{\bar{v}} \\ \bar{\bar{w}} \end{Bmatrix} = 0 \qquad (41)$$

The equations for the antisymmetric circumferential modes are identical to (41) except that the coefficients are replaced by their primed

counterparts described in Appendix I.

Programming of equations (41) allowed the maximum number of terms in the displacement series to be increased to 19 or a (57x57) eigenvalue problem. The eigenvalues and eigenvectors of (41) were calculated by the Jacobi rotation technique described briefly in Appendix III.

NUMERICAL RESULTS

The analysis developed in the previous section was used to calculate the natural frequencies of several configurations of stiffened and unstiffened shells for which frequencies are available in the literature.

Unstiffened Cylinders

The natural frequencies of unstiffened cylindrical shells with length-radius ratios of 1 and 10 were calculated with equations (41) for both the freely supported and the clamped-clamped end conditions. The freely supported case requires only a single term in the displacement series because each term in equations (30) is an exact solution. Seven terms in the displacement series were used for the clamped-clamped shell. The results agreed as closely as could be determined with the graphs of the exact solutions given by Fosberg (51).

A comparison of the analytical and experimental values of the natural frequencies of an unstiffened clamped-free cylinder is shown in Figure 4 and Table II. The theoretical frequencies were calculated with five of the axial mode functions of equations (32). Convergence of the frequencies was checked by increasing the number of terms to ten, which lowered the frequency (m=1, n=2) from 104.4 to 103.7 cps. The experimental values are taken from the report by Park et al (42). The shell geometrical and material properties are those of configuration 1 in Table I.

The fact that the discrepancy between the calculated and measured frequencies increases as the number of circumferential waves decrease indicates that the end conditions used in the analysis do not represent those of the experiment. This is due either to the assumed displacement

TABLE I SHELL CONFIGURATIONS USED IN NUMERICAL CALCULATIONS

Configuration	1[a]	2[b]	3	4[c]	5[c]
ρ_c, $\rho_{s\ell}$, ρ_{rk} [lb sec^2/in^4]	0.7332×10^{-3}	0.732×10^{-3}	0.732×10^{-3}	0.732×10^{-3}	0.732×10^{-3}
E_c, E_{rk}, $E_{s\ell}$ [lb/in^2]	0.30×10^{8}	0.30×10^{8}	0.30×10^{8}	0.30×10^{8}	0.30×10^{8}
ν	0.29	0.30	0.30	0.30	0.30
R(in)	0.10×10^{2}	0.7657×10	0.6×10	0.60×10	0.60×10
t(in)	0.30×10^{-1}	0.1826×10^{-1}	0.2×10^{-1}	0.15×10^{-1}	0.15×10^{-1}
a(in)	0.48×10^{2}	0.3885×10^{2}	0.12×10^{2}	0.24×10^{2}	0.24×10^{2}
$A_{s\ell}$(in^2)	0.3110×10^{-1}	0.1627×10^{-1}	0.30×10^{-1}	0.0	0.0
$\bar{z}_{s\ell}$(in)	-0.1376	-0.2082	0.125	0.0	0.0
$\bar{y}_{s\ell}$(in)	0.0	0.0	0.0	0.0	0.0
$I_{zzcs\ell}$(in^4)	0.1652×10^{-3}	0.1508×10^{-3}	0.2563×10^{-3}	0.0	0.0
$I_{yys\ell}$(in^4)	0.3895×10^{-3}	0.3744×10^{-3}	0.2563×10^{-3}	0.0	0.0
$I_{yzs\ell}$(in^4)	0.0	0.0	0.0	0.0	0.0
$(GJ)_{s\ell}$(lb in^2)	0.306×10^{3}	0.1131×10^{2}	0.2087×10^{4}	0.0	0.0
A_{rk} (in^2)	0.6251×10^{-1}	0.0	0.0	0.450×10^{-1}	0.451×10^{-1}
$\bar{z}_{rk}$ (in)	-0.1219	0.0	0.0	0.1955	0.0
$\bar{x}_{rk}$ (in)	0.0	0.0	0.0	0.0	0.0
I_{xxcrk}(in^4)	0.3253×10^{-3}	0.0	0.0	0.5274×10^{-3}	0.5978×10^{-3}
I_{zzcrk}(in^4)	0.4945×10^{-3}	0.0	0.0	0.54×10^{-4}	0.54×10^{-4}
I_{xzcrk}(in^4)	0.0	0.0	0.0	0.0	0.0
$(GJ)_{rk}$ (lb in^2)	0.5146×10^{4}	0.0	0.0	0.1981×10^{4}	0.2009×10^{4}

[a] Reference (42), Model 1S.

[b] Reference (17), 4 open profile stringers.

[c] Reference (39), Models 5 and 6.

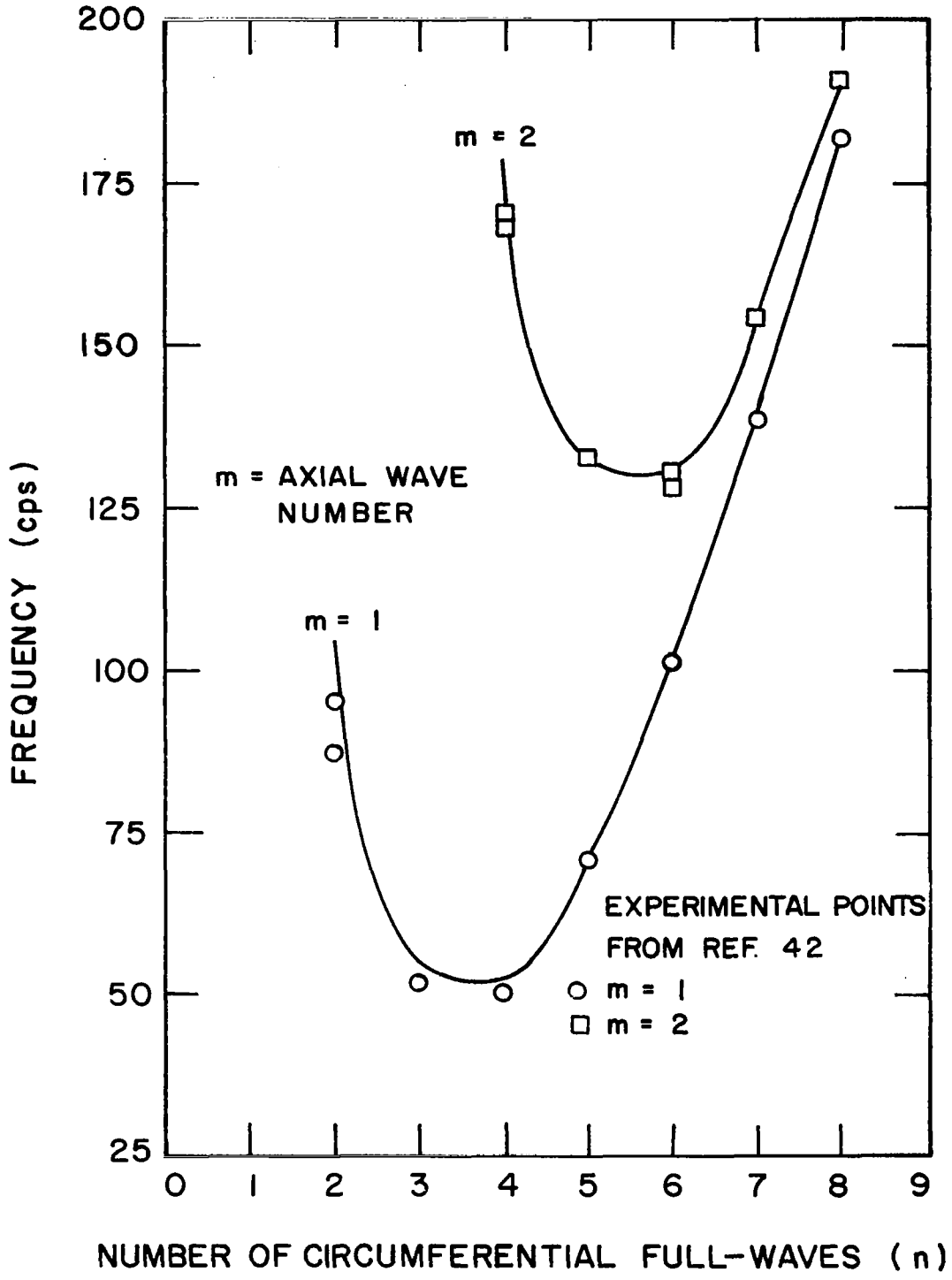

Figure 4. Theoretical and Experimental Frequencies of an Unstiffened Clamped-Free Cylindrical Shell

TABLE II

THEORETICAL AND EXPERIMENTAL FREQUENCIES OF AN OF AN UNSTIFFENED CLAMPED-FREE CYLINDER

n	m = 1		m = 2	
	Theory [a]	Exper. [b]	Theory	Exper.
2	104.4[c]	87.2 and 95.1		
3	55.6	51.5		
4	52.0	50.4	177.9	168.5 and 170.2
5		70.9		132.8
6		101.4		128.8 and 130.1
7	139.1	138.8	154.2	153.6
8	182.6	182.2	191.2	191.3

[a]Configuration 1, Table I.

[b]Reference (42), Model 1.

[c]Units are cycles/second.

functions not satisfying the free end conditions exactly or to the shell end not being rigidly clamped in the experiments. Since it is not necessary for the assumed displacements to satisfy force or moment end conditions (see reference 49) and since increasing the number of terms in the analysis affected the frequency at n=2 very slightly, it is concluded that the shell end was not absolutely fixed in the experiments.

Figure 5 and Table III show the theoretical and experimental frequencies of an unstiffened freely-supported cylindrical shell. The shell geometry and material properties are listed under configuration 4 in Table I. The cause of the discrepancy, which is as large as 28% at n=5, m=1, is, as was noted in reference (39), not known. However, the present theory agrees very well with the analysis of reference (39); hence it is concluded that an unaccounted-for factor in the experiments, perhaps an initial stress due to the welded seam in the shell, is responsible for the differences.

Stringer Stiffened Cylinders

Table IV compares some of the frequencies of a freely supported cylinder with four internal stringers computed with the present analysis ($m^*=1$, $n^*=6$) to those computed with the analysis of reference (46) and to a smeared analysis in reference (15). The material properties and geometry are listed under configuration 2 in Table I. The very slight differences in the frequencies of the present analysis (column a) and the complete analysis of reference (46) (column b) are due to the use of Flugge's shell theory and the inclusion of flexure and rotatory inertia of the stringers about the z-axis. The smeared analysis of Sewall and Naumann (15) shows very good agreement for this particular case.

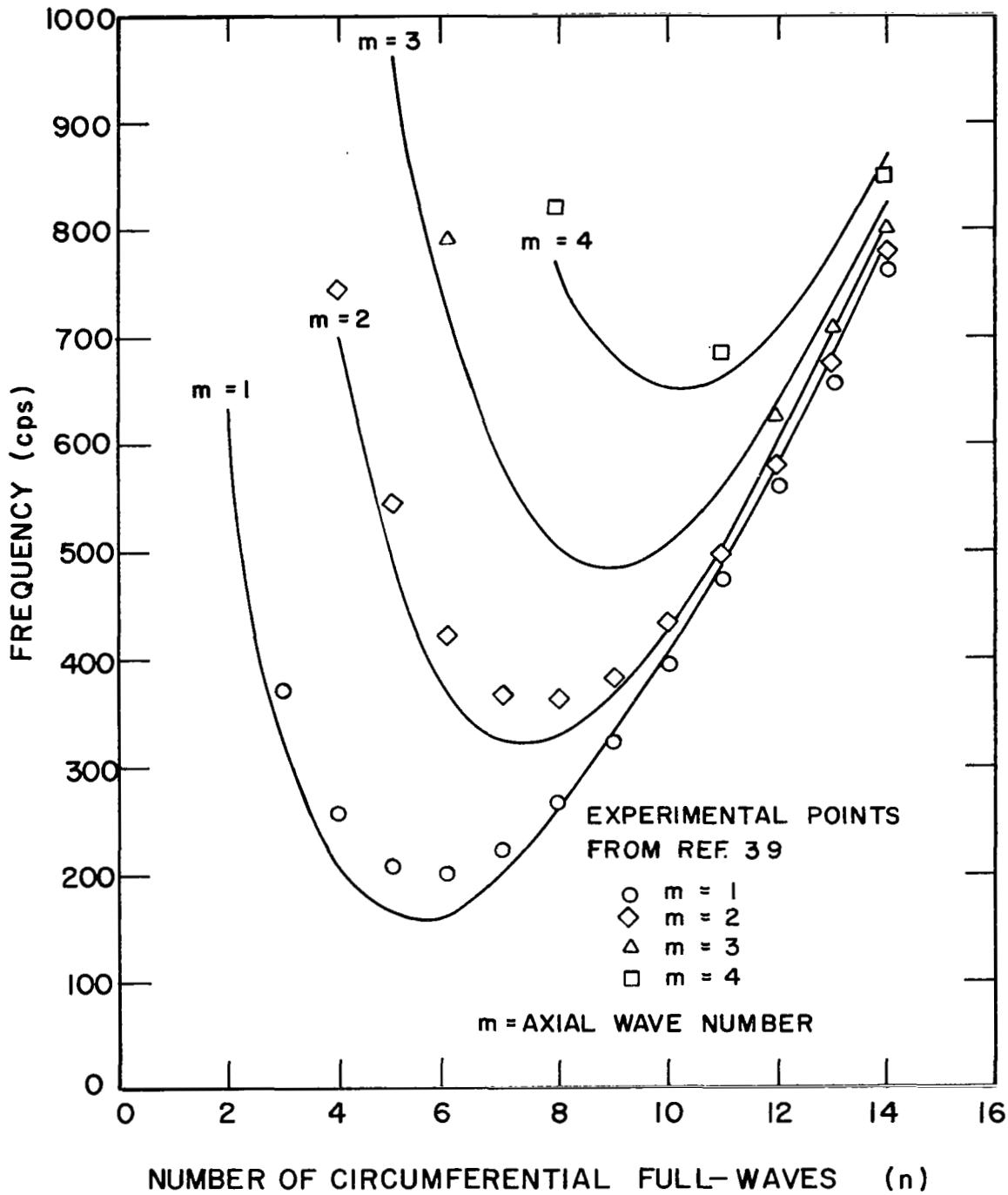

Figure 5. Theoretical and Experimental Frequencies of an Unstiffened Freely-Supported Cylindrical Shell

TABLE III

THEORETICAL AND EXPERIMENTAL FREQUENCIES OF AN UNSTIFFENED FREELY-SUPPORTED CYLINDER

N	m = 1		m = 2		m = 3		m = 4	
	Theory [a]	Exper. [b]	Theory	Exper.	Theory	Exper.	Theory	Exper.
2	633.5[c]							
3	326.7	370						
4	202.3	255	696.1	745				
5	159.9	205	483.0	545	960.6			
6	168.0	200	370.5	420	724.0	790		
7	206.0	220	325.1	345	580.8			
8	261.0	265	329.2	360	506.1		768.3	820
10	403.4	395	429.2	435	506.6		649.9	
12	581.1	560	594.9	580	632.3	625	706.4	
14	791.8	760	801.8	780	824.7	805	867.6	850

[a]Configuration 4, Table I.

[b]Reference (39), Model 1.

[c]Units are cycles/second.

TABLE IV

NATURAL FREQUENCIES OF A FREELY SUPPORTED CYLINDRICAL SHELL[a] WITH FOUR INTERNAL STRINGERS

M = 1	b		c		d		e
N	Sym	Antisym	Sym	Antisym	Sym	Antisym	Smeared
1	775.2[f]	775.2	775.2	775.2	1142.0	1124.0	774.4
2	318.0	314.5	318.1	314.6	360.2	361.5	315.4
3	158.4	158.4	158.8	158.8	169.4	168.3	158.3
4	99.3	102.6	100.5	104.0	102.8	108.2	101.0
5	90.7	90.7	92.9	92.9	94.7	95.0	90.8
6	105.7	111.3	108.3	114.2	109.4	116.5	108.6

[a]Configuration 2, Table I.

[b]Present Analysis.

[c]Analysis of reference 46, Donnell theory and in-surface inertias.

[d]Analysis of reference 46, deleting in-surface inertias.

[e]Analysis in reference 15, includes Novoshilov shell theory and in-surface inertias.

[f]Units are cps.

Figure 6 shows the variation of the minimum frequency of a stringer stiffened cylinder with the number of stringers. For the calculations, the total stringer area ($L\ A_{s\ell}$) and the "total" torsional stiffness ($L\ GJ_{s\ell}$) were held constant. This was done to compare the results of a discrete stiffener analysis to a smeared analysis which will give the same frequencies regardless of the number of stringers if ($L\ A_{s\ell}$) and ($L\ GJ_{s\ell}$) are constant. The stringers were taken to be identical and equally spaced around the circumference of the shell. The material and geometrical properties for the case with twelve stringers is listed under configuration 3 in Table I.

The analysis used for the calculations in Figure 6 is that of reference (46) with the in-surface inertias deleted. Thus, as can be seen in Table IV, the frequencies will be somewhat higher than those of a more exact analysis; but this is immaterial in comparing the effects of the number of stringers on the frequency.

The minimum frequency for each case shown in Figure 6 occurred for n=7 or 8 depending on the number of stringers. Both the symmetric and antisymmetric frequencies were calculated but only the smaller of the two was plotted.

It is interesting that there is a local maximum in the frequency for twelve stringers. This indicates that if a few stringers are to be used, there is a small advantage to choosing the proper number of stringers. However, at the present, the author does not know of a systematic procedure for determining this optimum number other than trial and error.

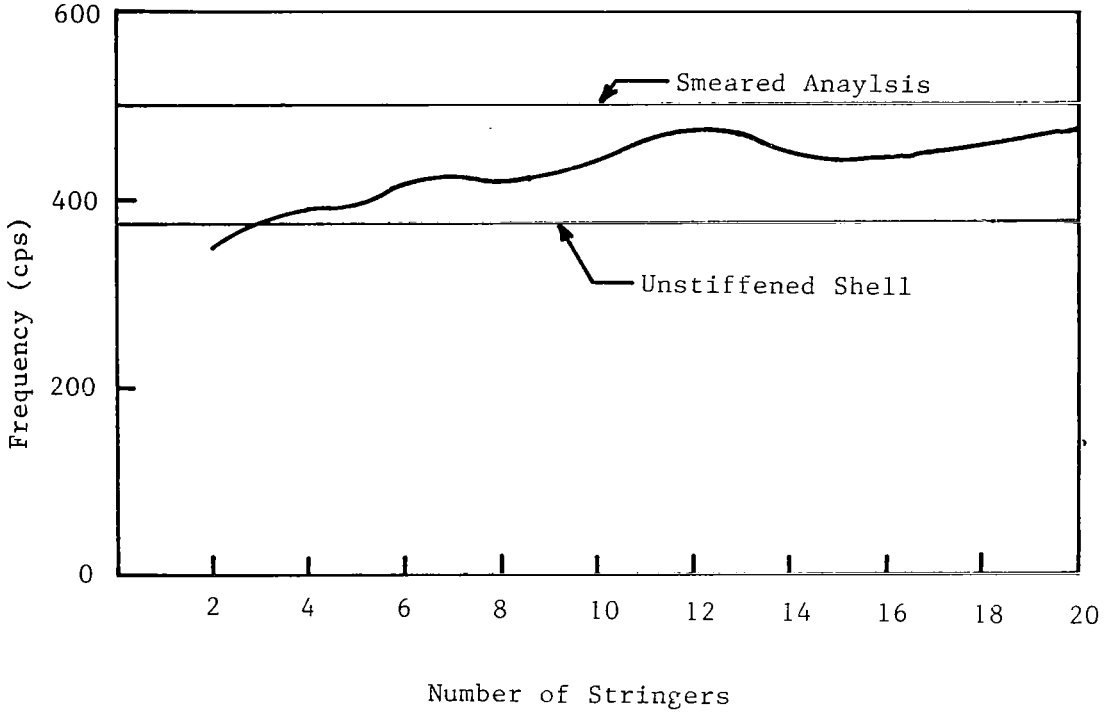

Figure 6. Minimum Frequency of a Cylindrical Shell as a Function of the Number of Stringers with the Total Stringer Area and Torsional Stiffness Constant

Ring Stiffened Shells

The natural frequencies for a cylinder with thirteen equally spaced rings is shown in Figure 7 and Table V. Frequencies were calculated for two cases, one with the ring cross section symmetric about the shell middle surface ($\bar{z}_{rk} = 0$) and the other with the rings external to the shell. These two cases correspond to models 5 and 6 in reference (39) and the material and geometrical properties are listed under configurations 4 and 5 in Table I. The results of the present analysis are compared to the analysis and experiments of reference (39), both of which showed very little difference between the external and symmetric rings.

In Figure 7, the frequencies labeled radial are the lowest frequencies associated with predominately radial motion in the shell. Likewise, axial and torsional correspond to the lowest frequencies associated with large u and v displacement components. Not shown are the other radial frequencies, many of which fall between the lowest radial and the lowest axial frequencies. For the higher values of n, many of the radial frequencies are very nearly the same as the lowest frequency. For example, for n=10, the twelve lowest frequencies lie between 2700 and 3100 cps for the external ring case.

The minimum (m=1) frequencies of this ring stiffened shell computed with the present analysis were compared to the frequencies calculated with the analysis of reference (46). The differences were found to be very slight, the maximum being on the order of 0.1%. These differences are due to the more exact shell theory and the inclusion of flexure and rotatory inertia of the rings about the z axis in the present analysis.

The lowest frequencies calculated with the present analysis also

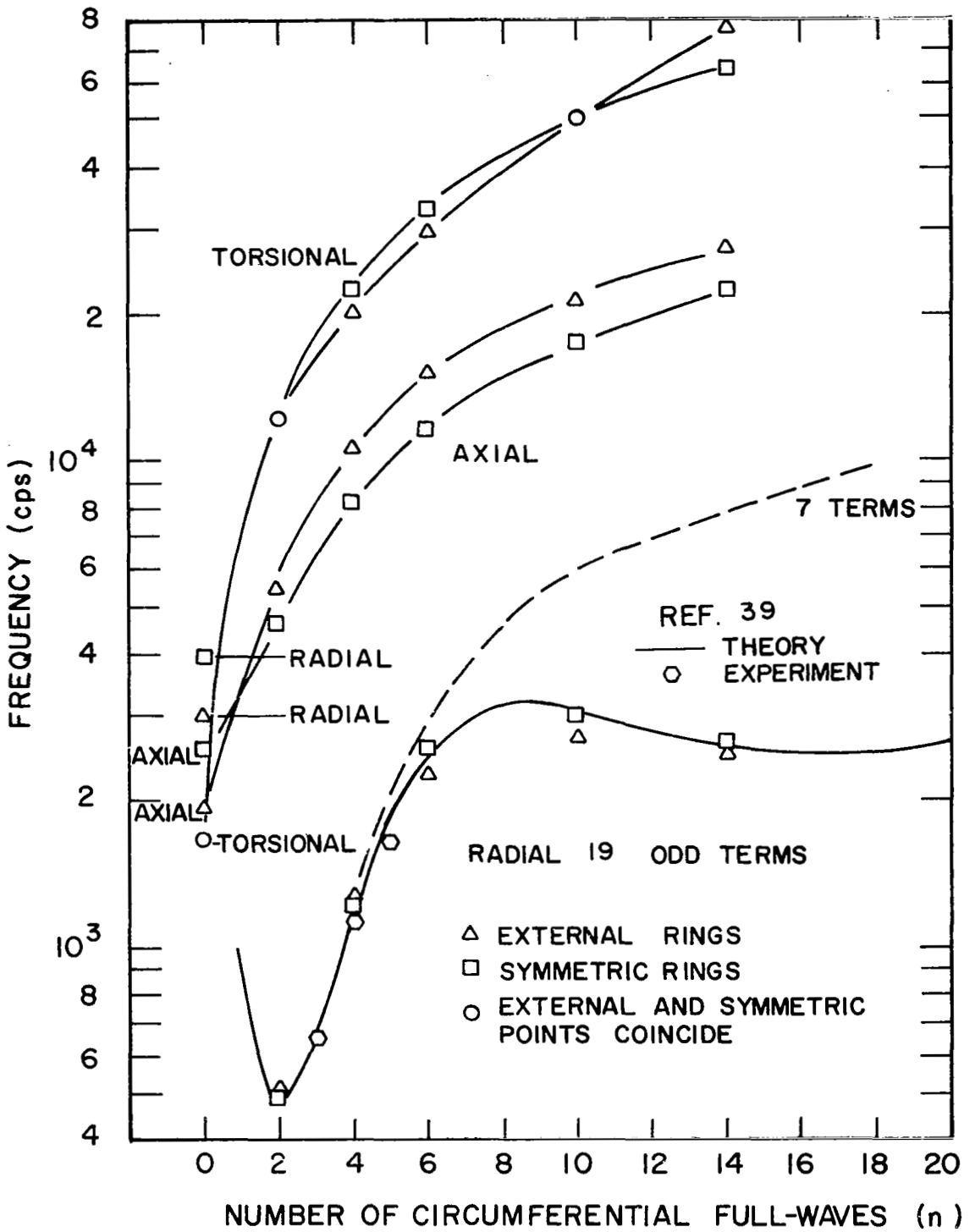

Figure 7. Theoretical and Experimental Frequencies of a Freely-Supported Cylindrical Shell with Thirteen Equally Spaced Rings

TABLE V

THEORETICAL FREQUENCIES OF A FREELY-SUPPORTED CYLINDER WITH THIRTEEN EQUALLY SPACED RINGS

N	Lowest Axial				Lowest Torsional				Lowest Radial			
	Ext. Rings[a]		Sym. Rings[b]		Ext. Rings		Sym. Rings		Ext. Rings		Sym. Rings	
	m	Theory	m	Theory	m	Theory	m	Theory	m	Theory	m	Theory
0	1	1926.4[c]	1	2542.1	1	1651.0	1	1649.7	27	2969.5	33	3953.4
2	1	5461.3	1	4625.7	1	12,347	1	12,362	1	518.3	1	490.7
4	1	10,447	1	8190.5	7	20,131	1	22,477	1	1287.5	1	1225.7
6	1	14,989	1	11,612	11	29,807	1	33,295	1	2276.7	1	2556.1
10	1	21,159	1	17,522	13	50,395	13	50,491	1	2694.8	1	2995.6
14	1	27,329	1	22,590	5	77,870	15	64,397	1	2506.8	1	2601.4

[a]Configuration 4, Table I.

[b]Configuration 5, Table I.

[c]Units are cycles/second.

compare very well with the theory of reference (39) for the symmetric rings. However, the present analysis predicts a very definite effect due to the eccentricity of the rings. The frequencies for the external rings are higher than those for the symmetric rings for $n<4$ and the opposite is true for $n>4$.

In order to achieve agreement between the two theories for the symmetric rings, it was necessary, because of computer size limitations, to take advantage of the longitudinal symmetry in this problem. It may be shown that if the shell ring configuration is symmetric about the $x = a/2$ plane, then the odd axial modes ($m = 1, 3, 5, \ldots$) uncouple from the even axial modes ($m = 2, 4, 6, \ldots$). This allows the frequencies in each case to be calculated independently, thereby doubling the maximum number of terms in the displacement series for the same computer storage.

For the calculations in Figure 7, $m^* = 19$ and $n^* = 1$, but since only the odd terms $m = 1, 3, 5, \ldots$) were used in the displacement series, the highest value of m is 38. Also shown are the lowest frequencies for a seven term series which is obviously inadequate to describe the motion for large values of n. The following shows the lowest radial frequencies (cps) for $n = 4$ calculated with three progressively larger displacement series for the symmetric ring case.

Range of m	Frequency
1 - 7	1758.1
1 - 19 odd only	1758.1
1 - 37 odd only	1225.7
Theory of ref. (39)	1180.

This illustrates very well one of the pitfalls of an assumed modes method

such as Rayleigh-Ritz. The frequency for m = 1-7 appears to be converged when it is actually 50% high.

Figures 8 - 11 show the normalized radial displacement modes as a function of x/a, the axial coordinate. The rings are located at x/a = k/12, k = 0, ..., 12. The eigenvectors, from which these plots are derived, indicate that for n = 2, there is little coupling between the predominant term in the displacement series and the remaining terms; while for n = 10, there is strong coupling between several terms in the series. The mode associated with the lowest frequency for n = 10, Figure 11, has the three largest terms

$$w(x) = \sin(\pi x/a) + 0.473 \sin(23\pi x/a) - .466 \sin(25\pi x/a)$$

the remainder of the coefficients being less that 2% of the largest. The interesting point about this eigenfunction is that even though it consists almost entirely of the 1st, 23rd and 25th axial modes of the unstiffened shell, they are combined in such a way that none of the predominant terms is recognizable. If this modal function was being determined experimentally, it could easily be mistaken for the n = 10, m = 12 mode.

In order to check the validity of neglecting the torsional, torsional-flexural, and torsional-extensional contributions to the normal strain energy, several of the terms which have been omitted from equations (23) were added to the analysis and the frequencies of the ring stiffened shell were recalculated. The added terms, which are the only non zero terms in the second integral of equation (23) for rings whose cross sections are symmetric about the z-axis, are

$$\frac{E_{rk}}{2} \int_0^{2\pi} \left[\frac{\Gamma_{rk}}{R^3} w_{,x\theta\theta}^2 - \frac{2}{R^3} \hat{z}_{rk} I_{zzrk} u_{,\theta\theta} w_{,x\theta\theta} + \frac{2}{R^2} \hat{z}_{rk} I_{zzrk} w_{,x} w_{,x\theta\theta} \right]_{x=x_k} d\theta$$

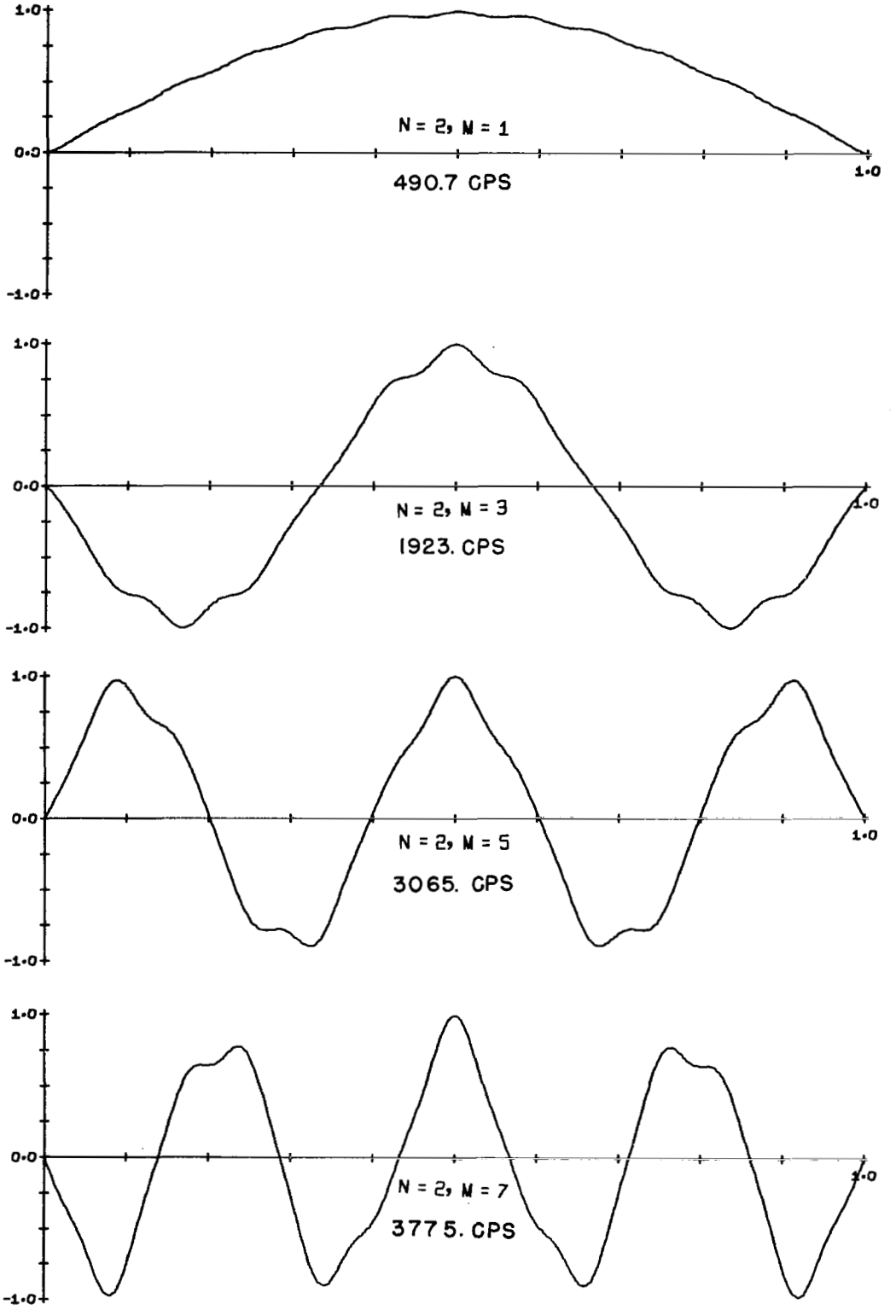

Figure 8. Theoretical Axial Modes of a Freely-Supported Cylinder with Thirteen Equally Spaced Symmetric Rings (N=2)

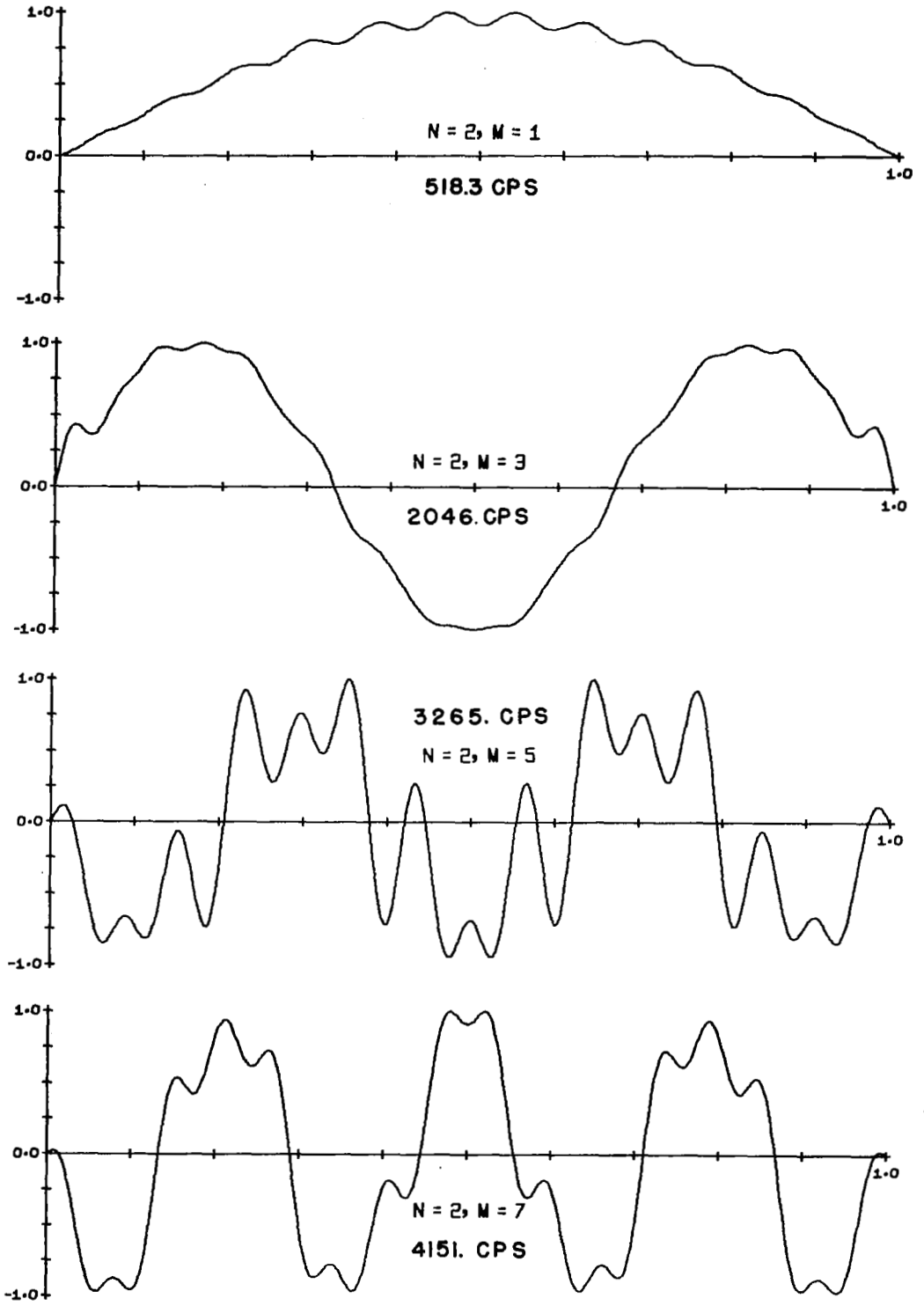

Figure 9. Theoretical Axial Modes of a Freely-Supported Cylinder with Thirteen Equally Spaced External Rings (N=2)

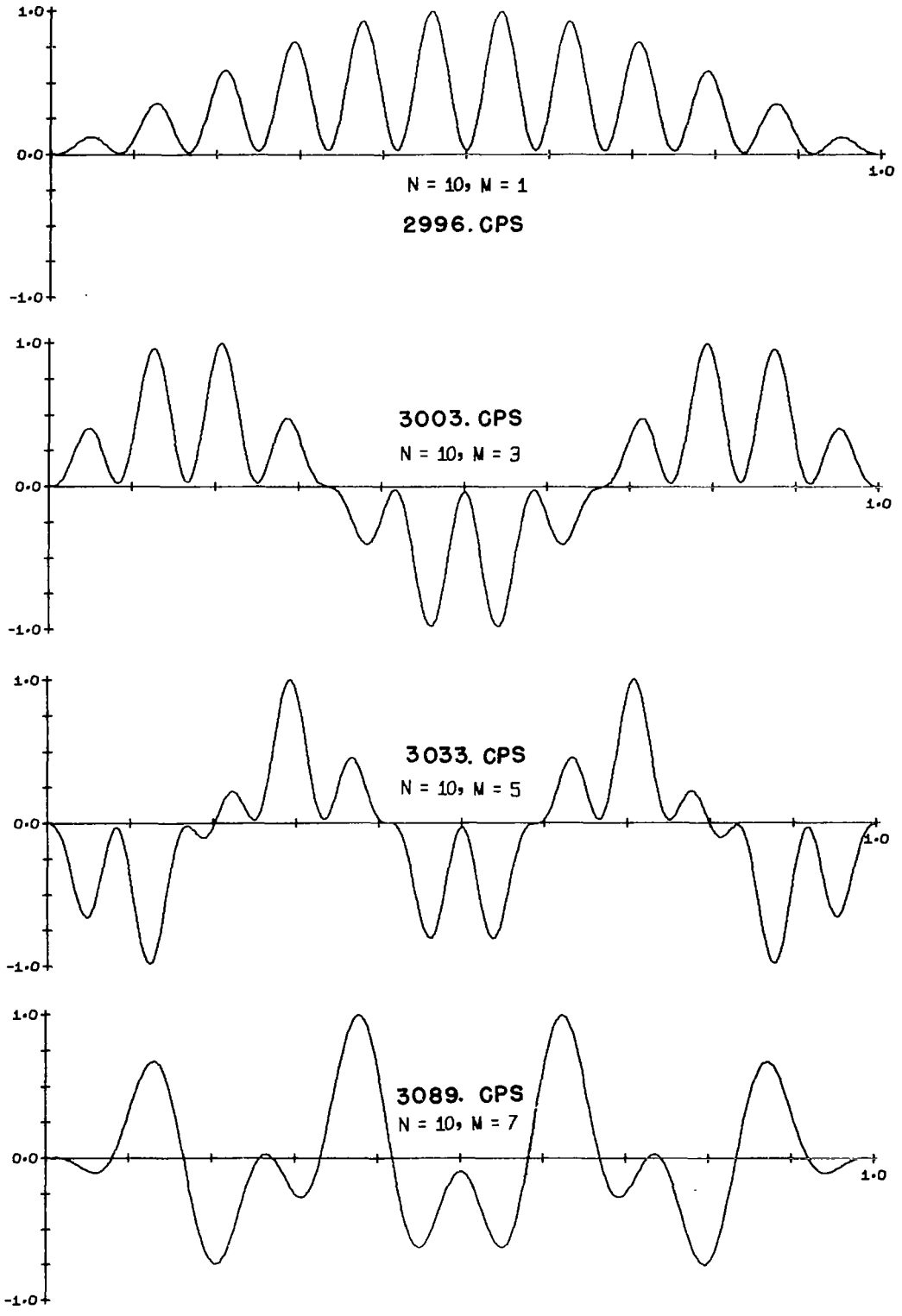

Figure 10. Theoretical Axial Modes of a Freely-Supported Cylinder with Thirteen Equally Spaced Symmetric Rings (N=10)

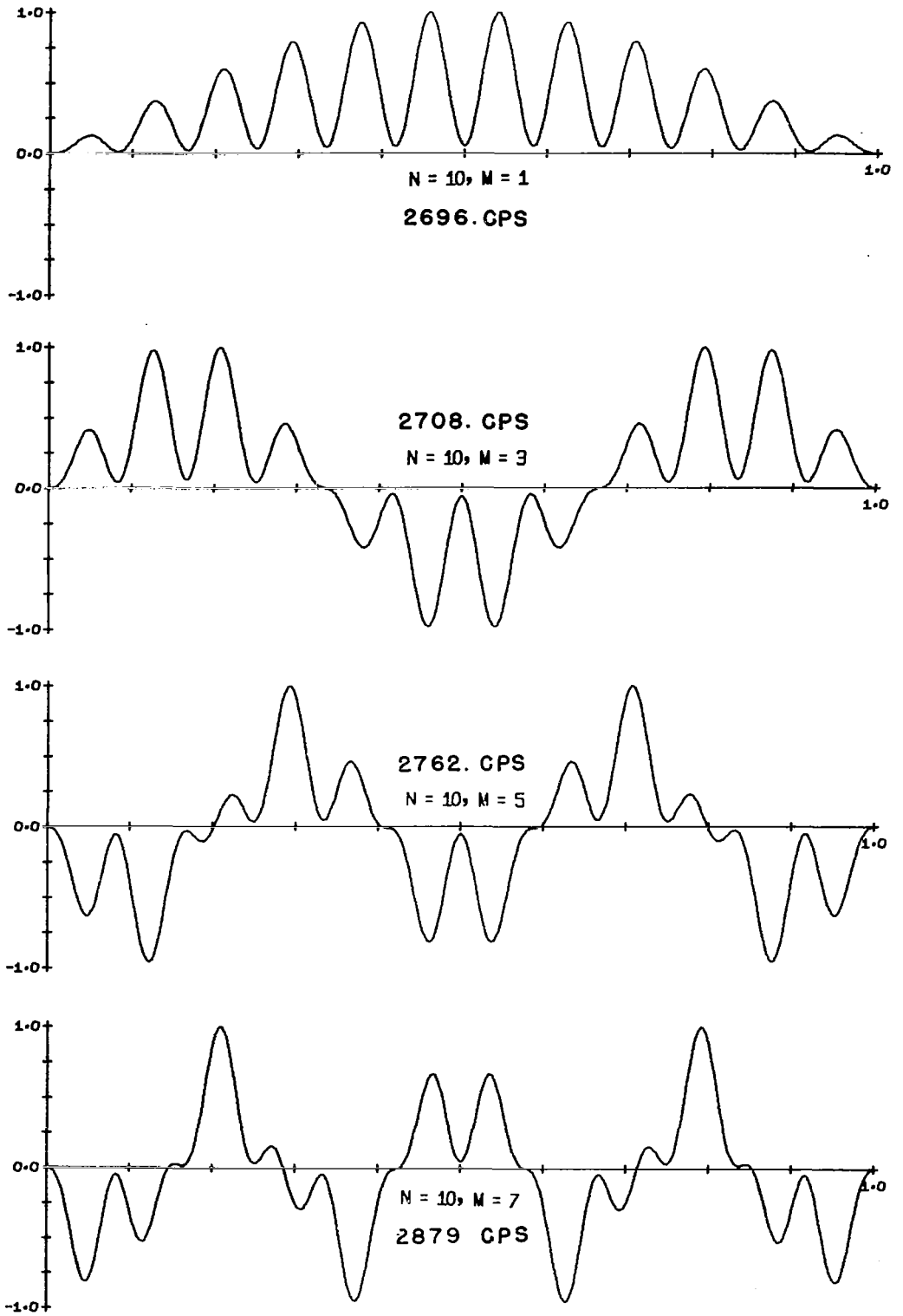

Figure 11. Theoretical Axial Modes of a Freely-Supported Cylinder with Thirteen Equally Spaced External Rings (N=10)

where $\Gamma_{rk} = I_{zzrk}\,\bar{z}^2_{rk}$

$\hat{z}_{rk} = \bar{z}_{rk}$

for symmetric ring cross sections. These terms produced a change in the lowest natural frequency for N=6, 10 of less than 0.4%. The changes in the three lowest frequencies were all less than 1%.

A few calculations of the frequencies of a clamped-clamped ring stiffened shell were carried out for comparison with the experiments in reference (7). The results are shown in Table VI. In the experiments the rings on the ends of the shell were clamped, and even if the clamping was not rigid, one would expect the frequencies to be higher than the freely supported case. At the present, it is not known why the calculated frequencies for the freely supported end conditions are higher than the experiments.

Ring and Stringer Stiffened Shell

The natural frequencies and normal modes for a clamped-free cylindrical shell with three internal rings and sixteen internal stringers were calculated with the present analysis. The rings are equally spaced and located at x/a = 1/3, 2/3, 1 and the stringers are equally spaced around the circumference. The material and geometrical properties are listed in Table I under configuration 1.

The axial mode functions used were those of equations (32). The following tabulation shows the lowest natural frequency (cps) for three different ranges of m.

TABLE VI

NATURAL FREQUENCIES OF A CYLINDER WITH SEVEN EXTERNAL RINGS

M=1

N	a	b	c	d
3	616[e]	503	494	378-441
4		650		580,600
5		861	809	760

a Clamped-clamped 1-13 terms.

b Freely supported 1-13 terms.

c Freely supported 1-19 odd terms.

d Experiment, taken from reference (7).

e Units are cycles/second.

Range of m	n=3	n=8
1 - 3	144.0	483.3
1 - 10	135.2	264.3
1 - 19	130.3	263.5

The range m = 1-10 gives values reasonably close to those for m = 1-19 and was judged sufficient for further calculations.

Figure 12 and Table VII show a comparison of natural frequencies calculated with the present analysis to the experimental values given by Park et al (42). The calculated values are those associated with the symmetric circumferential modes and the coupling between the circumferential modes was ignored (only a single term was used in the circumferential modal series). Note that the order of increasing frequency (for constant n) is not necessarily the same as increasing axial mode number, m. The axial mode number associated with each frequency is determined as in reference (46) by the m value associated with the predominant term in the eigenvector.

The validity of neglecting the circumferential modal coupling was checked by reducing the number of axial modes and including several circumferential modes. Two cases were run, one with the ranges m = 1-3, n = 1-4 and the other with m = 1-3, n = 6-10. In the first case, there was no effect of including the extra circumferential terms, which is in agreement with a conclusion reached in reference (46), that is, the coupling between two circumferential modes, j and n, is zero if j + n is less than the number of equally spaced stringers. In the second case, there was coupling between n = 6 and 10 and n = 7 and 9 but it was not appreciable and would have very little effect on the frequencies.

The cause of the discrepancy between the theory and experiment in

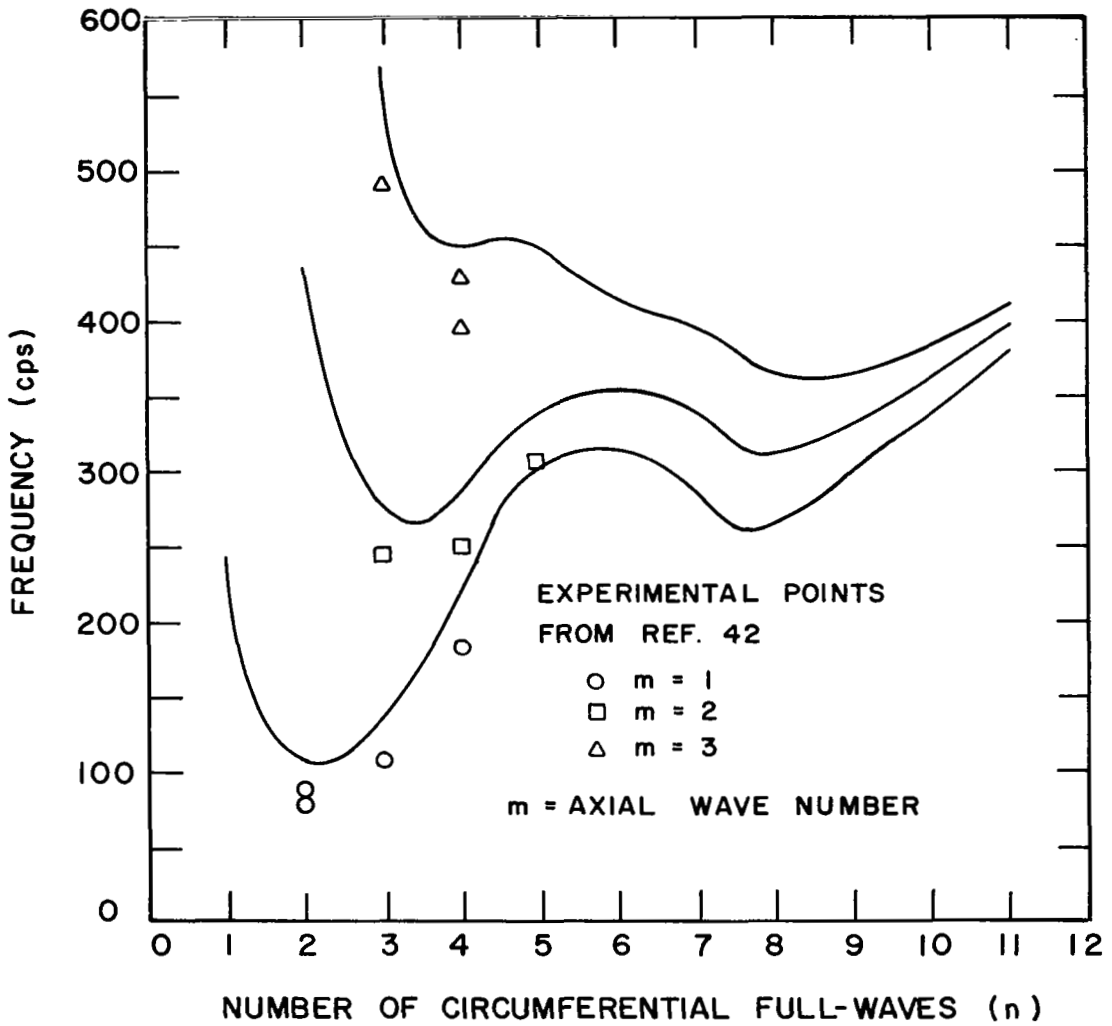

Figure 12. Theoretical and Experimental Frequencies of a Clamped-Free Cylindrical Shell with Three Rings and Sixteen Stringers

TABLE VII

THEORETICAL AND EXPERIMENTAL FREQUENCIES OF A CLAMPED FREE CYLINDER WITH THREE RINGS AND SIXTEEN STRINGERS

N	First Frequency			Second Frequency			Third Frequency		
	m	Theory[a]	Exper.[b]	m	Theory	Exper.	m	Theory	Exper.
1	1	243.9[c]							
2	1	105.8	80.2 and 88.2	2	433.9				
3	1	135.2	107.5	2	274.1	246.2	3	568.2	491.8
4	1	216.9	184.6	2	285.9	251.5	3	447.1	397.0 and 430.4
5	1	302.5		2	333.2	304.6	3	445.9	
6	2	315.0		1	353.8		4	414.0	
7	4	286.0		1	340.2		2	394.0	
8	4	264.3		1	310.6		2	361.3	
9	4	300.9		1	332.7		6	367.7	
10	4	334.4		1	357.4		6	380.2	
11	4	378.1		5	395.8		6	409.2	

[a]Configuration 1, Table I.

[b]Reference (42), Model 1S.

[c]Units are cycles/second.

Figure 12 is not known at the present time. It is possibly due to the neglect of an axial mode other than m = 1-19 or the assumption of the small ring depth to radius ratio used in equations (18, 19, and 20). The end conditions, both those used in the experiments and the analysis, could be partially responsible for the error in the lowest frequencies (as was concluded to be the cause of discrepancy in Figure 4) but would not affect the higher frequencies.

Figures (13-15) show a few of the radial deflection normal mode functions associated with the frequencies in Figure 12. As was noted in the discussion of the modes of the thirteen ring-stiffened shell, the eigenvectors, from which Figures (13-15) are derived, indicate that for n = 2 there is little coupling between the predominant term in the displacement series and the remaining terms, while for the higher n values, there is strong coupling between the largest term (the value of m given in the figure) and several other terms in the series. The mode shapes also show a pronounced increase in shell motion (compared to the rings) at the high values of n.

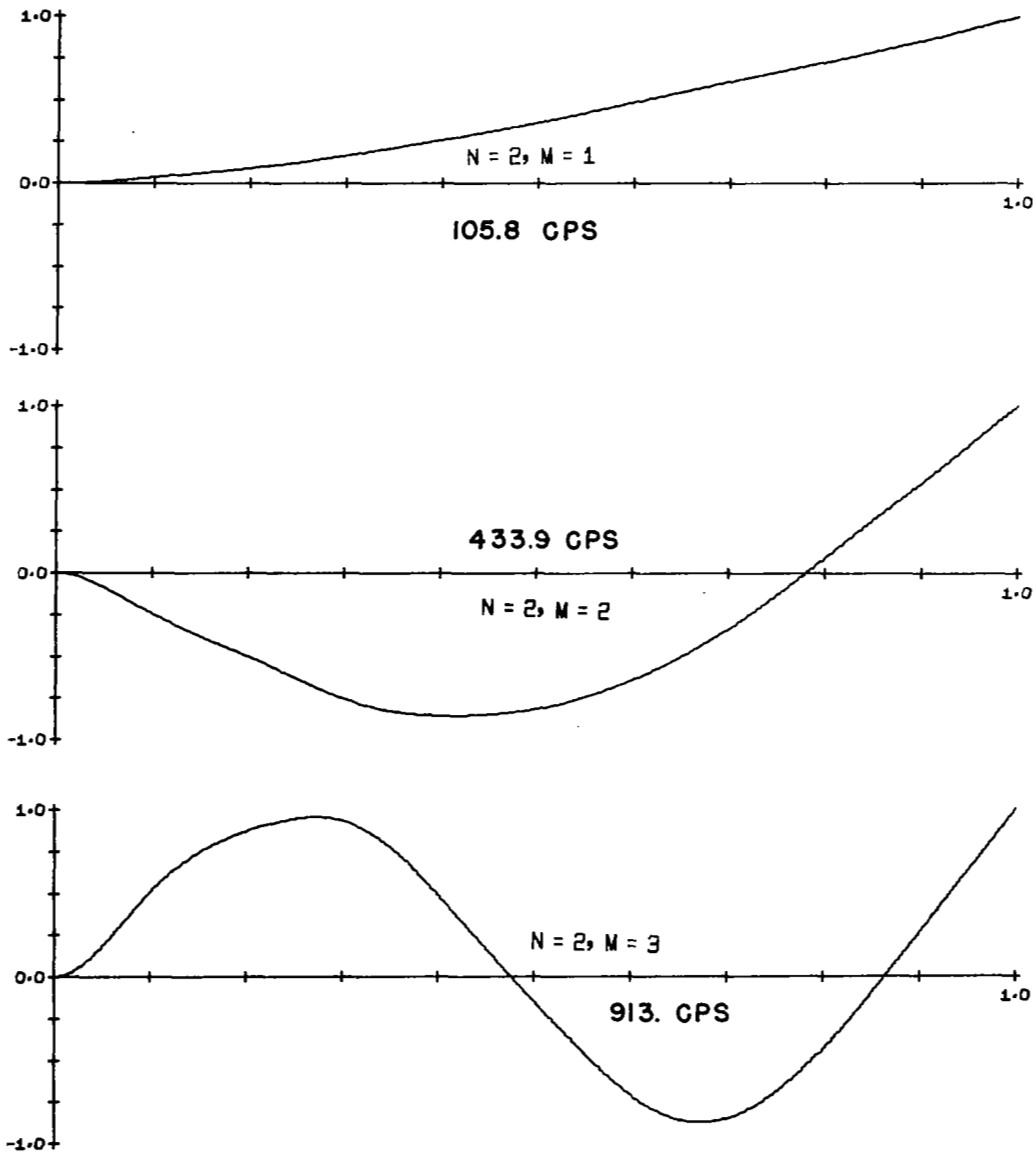

Figure 13. Theoretical Axial Modes of a Clamped-Free Cylinder with Three Rings and Sixteen Stringers (N=2)

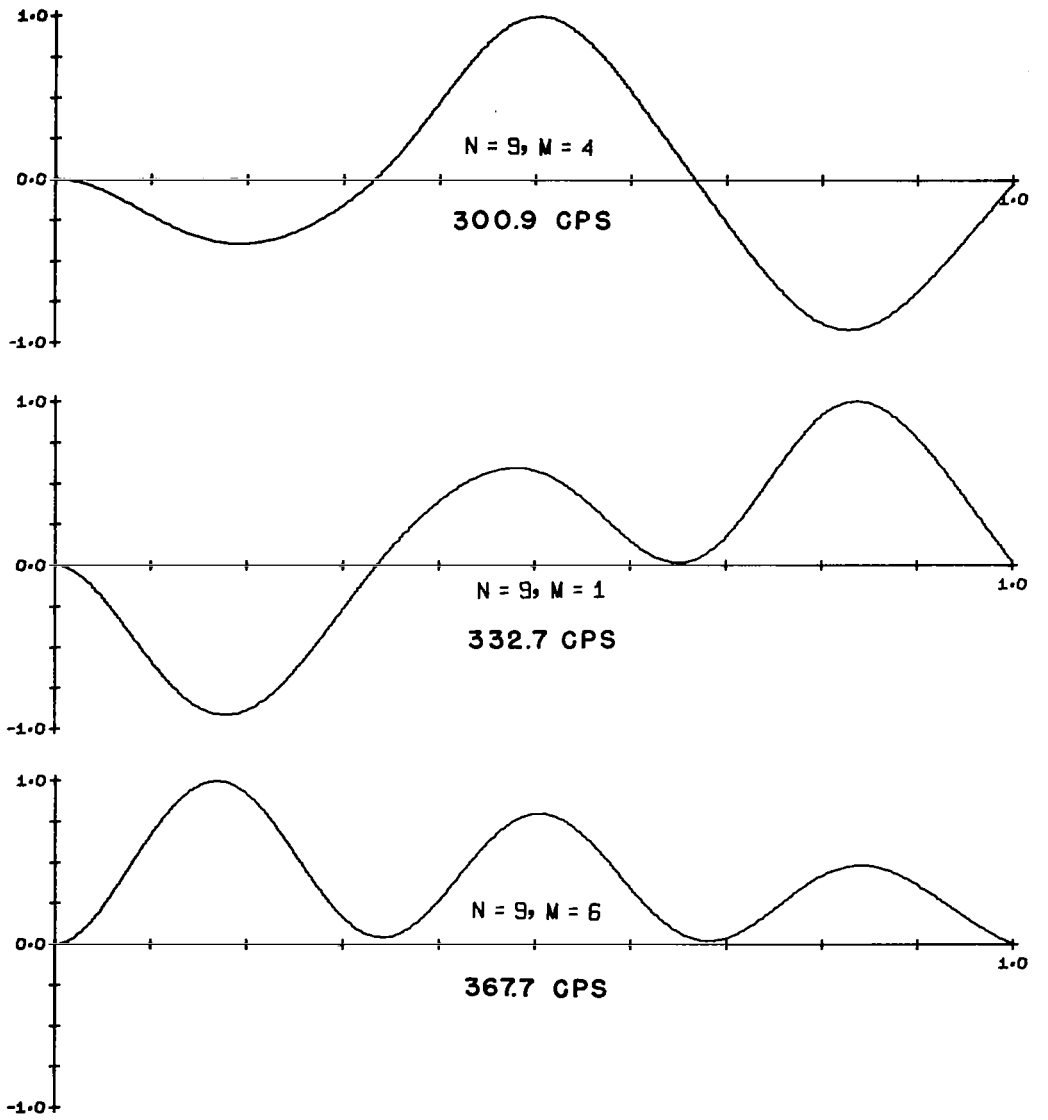

Figure 14. Theoretical Axial Modes of a Clamped-Free Cylinder with Three Rings and Sixteen Stringers (N=9)

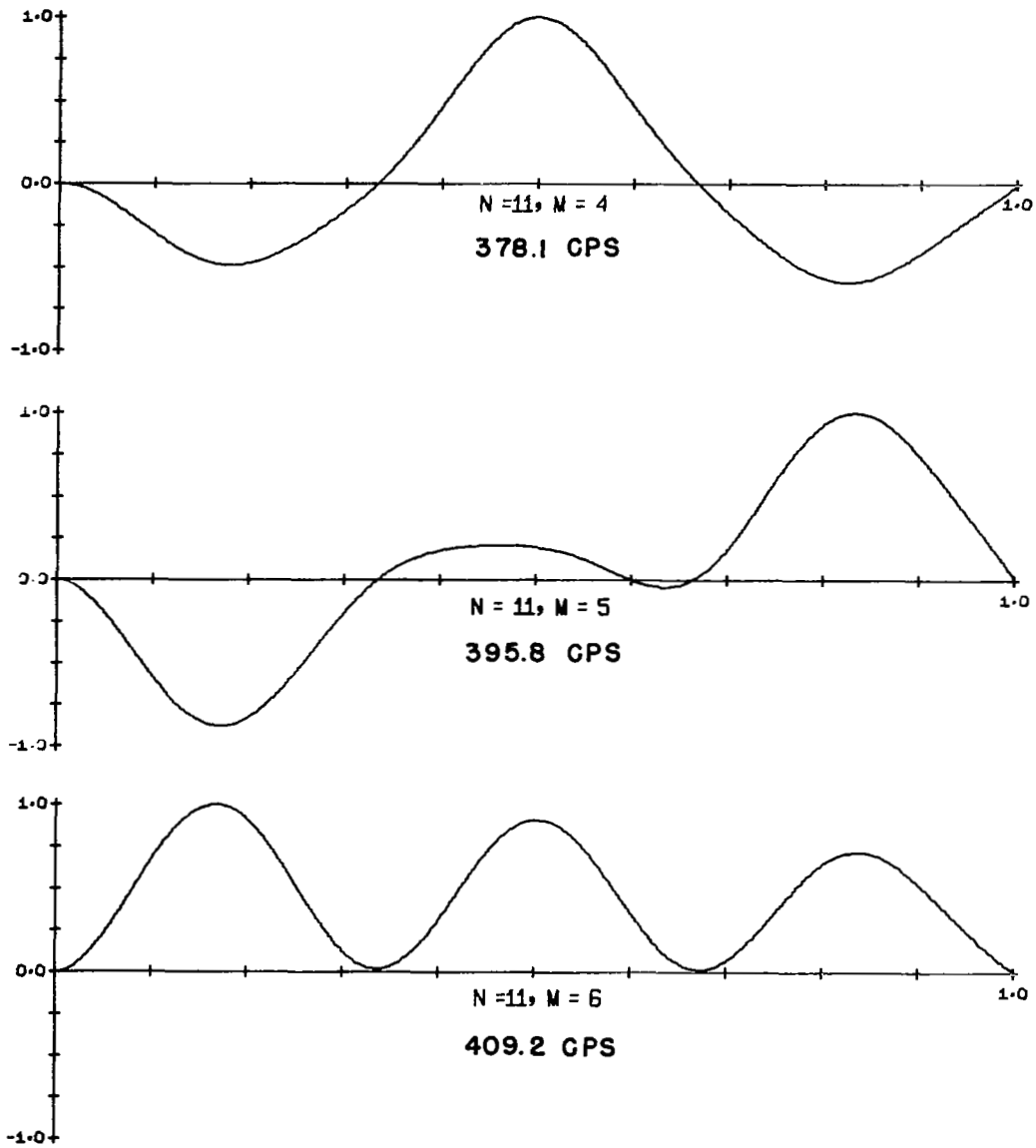

Figure 15. Theoretical Axial Modes of a Clamped-Free Cylinder with Three Rings and Sixteen Stringers (N=11)

CONCLUDING REMARKS

A theoretical analysis for the free vibration of ring and stringer stiffened shells, with stiffeners treated as discrete elements has been developed and implemented for digital computer solution. The analysis is capable of handling arbitrary end conditions and arbitrary distributions of stiffeners. Comparison of numerical results with experiments and other analyses show good agreement for stringer stiffened shells and reasonable agreement for ring stiffened shells.

The Rayleigh-Ritz technique for calculating the natural frequencies of discretely stiffened cylinders produces acceptable results. However, use of the solutions for the unstiffened shell as the assumed displacements yields an unusually large and unwieldy eigenvalue problem whose convergence may be erratic or, at least, unusual. It is the author's suggestion that further study be directed toward developing displacement functions which allow for inter-stiffener deformation with the expectation of reducing the numerical problem for the same accuracy.

The question of the effect of ring eccentricity is not, in the author's opinion, resolved. The work of Hu, Gomerly, and Lindholm indicates there is very little effect in the frequencies due to ring eccentricity. The present analysis and the analyses of Sewall and Naumann, and Mikulas and McElman indicate there is a definite effect. Perhaps experiments with integral or welded ring-shell construction and designed to exaggerate the eccentricity effect would settle the issue. It should also be noted that the experiments of Hu, Gormerly and Lindholm only indirectly verified the existence of the second minimum in the frequency vs. n curve (they reported numerous frequencies which

could not be identified in this region which is consistent with the theoretical results).

The contributions of the more exact shell theory and the flexure and rotatory inertia of the stiffeners about the z-axis show very little effect on the frequencies on the configurations of stiffened shells considered in this report. Likewise, the contributions of extension due to torsion and the torsion-extension, torsion-flexure coupling in the rings is insignificant. Unless geometries considerably different that those considered here are used, these minor refinements only increase the complexity of the analysis with negligible increase in accuracy in the results.

REFERENCES

1. Hoppmann, W.H., II, "Flexural Vibrations of Orthogonally Stiffened Cylindrical Shells", Proc. 9th International Congress of Applied Mechanics, Bruxelles, pp. 225-237 (1956).

2. Hoppmann, W.H., II, "Some Characteristics of the Flexural Vibrations of Orthogonally Stiffened Cylindrical Shells", J. Acous. Soc. Amer., vol. 30, pp. 77-82 (1958).

3. Nelson, H.C., B. Zapotowski and M. Bernstein, "Vibration Analysis of Orthogonally Stiffened Circular Fuselage and Comparison with Experiments", Proc. National Specialists Meeting on Dynamics and Aeroelasticity, Fort Worth, Texas, pp. 77-87 (Nov. 1958).

4. Foxwell, J.H. and R.E. Franklin, "The Vibrations of a Thin-Walled Stiffened Cylinder in an Acoustic Field", Aero. Quart., vol. 10, pp. 47-64 (1959).

5. Miller, P.R., "Free Vibrations of a Stiffened Cylindrical Shell", Aeronautical Research Council Reports and Memoranda No. 3154, London (1960).

6. Bleich, H.H., "Approximate Determination of the Frequencies of Ring-Stiffened Cylindrical Shells", Osterreichisches Ingenieur-Archiv, vol. 15, No. 1-4, pp. 6-25 (1961).

7. Sewall, J.L., R.R. Clary and S.A. Leadbetter, "An Experimental and Analytical Vibration Study of a Ring-Stiffened Cylindrical Shell Structure with Various Support Conditions", NASA TN-D-2398, (Aug. 1964).

8. Levy, R.S. and R.E. Jewell, "Dynamic Response of Pressurized Stiffened Cylinders with Attached Concentrated Masses", AIAA Symposium on Structural Dynamics and Aeroelasticity, Boston, Mass., pp. 316-328 (Aug. 30 - Sept. 1, 1965).

9. Weingarten, V.I., "Free Vibrations of Ring Stiffened Conical Shells," AIAA Jour., vol. 3, pp. 1475-1481 (1965).

10. Mikulas, M.M., Jr. and J.A. McElman, "On the Free Vibration of Eccentrically Stiffened Cylindrical Shells and Plates", NASA TN-D 3010 (Sept. 1965).

11. Diet, W.K., "On the Formulation of Equations of Motion of an Eccentrically Stiffened Shallow Circular Cylindrical Shell", Syracuse Univ. Research Institute Report No. 1620.1245-47 (Feb. 1966).

12. McElman, J.A., M.M. Mikulas, Jr., and M. Stein, "Static and Dynamic Effects of Eccentric Stiffening of Plates and Shells", J. AIAA, vol. 4, No. 5, pp. 887-894, (May 1966).

13. McElman, J.A., "Eccentrically Stiffened Shallow Shells", Ph.D. Dissertation, Virginia Polytechnic Institute, Blacksburg, Va. (June 1966).

14. Resnick, B.S. and J. Dugundji, "Effects of Orthotropicity, Boundary Conditions, and Eccentricity on the Vibrations of Cylindrical Shells", MIT Aeroelastic and Structures Laboratory, AFOSR Scientific Report AFOSR 66-2821, AD648077 (Nov. 1966).

15. Sewall, J.L. and E.C. Naumann, "An Experimental and Analytical Vibration Study of Thin Cylindrical Shells with and without Longitudinal Stiffeners", NASA TN D-4705 (1968).

16. Schnell, W. and F.J. Heinrichsbauer, "Zur Bestimmung der Eigenschwingungen Langsversteifter, Dunnwandiger Kreiszlinderschalen", Jahrbuch Wissenschaft, Ges. Luft u. Raumfehrt (WGLR), pp. 278-286, (1963).

17. Schnell, W. and F. Heinrichsbauer, "The Determination of Free Vibrations of Longitudinally-Stiffened Thin-Walled, Circular Cylindrical Shells", NASA TT F-8856 (April 1964).

18. Bartolozzi, G., "Vibrazioni Proprie Dei Gusci Irrigiditi", Aerotecnia, vol. 46, pp. 3-17 (1966).

19. Ojalvo, I.V. and M. Newman, "Natural Vibrations of a Stiffened Pressurized Cylinder with an Attached Mass", AIAA Jour., vol. 5, No. 6 (June 1967).

20. McDonald, D., "Free Vibration of Stiffened Cylindrical Shells", Final Report NASA Contract No. NAS8-20391, NASA CR-91777 (Oct. 1967).

21. Galletly, G.D., "On the In-Vacuo Vibrations of Simply Supported Ring-Stiffened Cylindrical Shells", Proc. 2nd U.S. National Congress of Applied Mechanics, ASME, pp. 225-231 (1955).

22. Gondikas, P., "Vibrations of Ring Stiffened Shells", Columbia University, Dept. of Civil Engineering and Engineering Mechanics, Contract No. Nonr 266(08), Tech. Report 13, AD67036 (Mar. 1955).

23. Baron, M.L., "Circular Symmetric Vibrations of Infinitely Long Cylindrical Shells with Equidistant Stiffeners", J. Appl. Mech., vol. 23, pp. 316-318 (1956).

24. Galletly, G.D., "Flexural Vibrations of Stiffened Cylinders", Jour. Acous. Soc. Amer., vol. 30, p. 644 (1958).

25. Paslay, P.R., E.K. Walsh, and D.F. Muster, "Program Write-Up for Determination of Vibration Response of a Ring-Stiffened Cylindrical Shell", General Electric Co., General Engineering Laboratory Report 60GL147 (1960).

26. Paslay, P.R., E.K. Walsh, and D.F. Muster, "Field Equations for Underwater Sound Propagated by Ring-Stiffened Cylindrical Shells", General Electric Co., General Engineering Laboratory Report 60GL51 (1960).

27. Wernick, R.J. and D.F. Muster, Addendum to "Field Equations for Underwater Sound Propagated by Ring-Stiffened Cylindrical Shells", General Electric Co., General Engineering Laboratory Report 60GL51-A (July 1960).

28. Tatge, R.B., "Analysis of Measured Vibrational Modes of a Ring-Stiffened Cylindrical Shells", General Electric Co., General Engineering Laboratory Report 61GL106, AD258790 (1961).

29. Tatge, R.B., "Underwater Sound Propagation by Ring-Stiffened Cylindrical Shells", General Electric Co., General Engineering Laboratory Report 62GL146, AD287198 (1962).

30. Garnet, H. and M.A. Goldberg, "Free Vibrations of Ring-Stiffened Shells", Grumman Aircraft Research Report RE-156 (March 1962).

31. McGrattan, R.J. and E.L. North, "Shell Mode Coupling", General Dynamics Corp., Electric Boat Division Report U411-63-005, AD409454 (1963).

32. McGrattan, R.J., E.L. North, and C.P. Tsokos, "Shell Mode Coupling", David Taylor Model Basin Contract Nonr 3594(00), AD600958 (1963).

33. Wah, T., "Circular Symmetric Vibrations of Ring-Stiffened Cylindrical Shells", J. Soc. Indust. Appl. Math., vol. 12, pp. 649-662 (1964).

34. Yao, J.C., "On the Response of Rocket Vehicle Structure to Certain Environmental Loads", 35th Symposium on Shock and Vibration, New Orleans, La., pp. 1-8 (Oct. 25-28, 1965).

35. Wah, T., "Flexural Vibrations of Ring-Stiffened Cylindrical Shells", Jour. of Sound and Vibration, vol. 3, pp. 242-251 (1966).

36. Godzevich, V.G. and O.V. Ivanova, "Free Oscillations of Circular Conical and Cylindrical Shell Reinforced by Rigid Circular Ribs", NASA TT F-291 (Feb. 1965).

37. Ory, H., E. Hornung and G. Fahlbusch, "A Simplified Matrix Method for the Dynamic Examination of Different Shells of Revolution", AIAA Symposium on Structural Dynamics and Aeroelasticity, Boston, Mass., pp. 365-368 (Aug. 30 - Sept. 1, 1965).

38. Bushnell, D., "Axisymmetric Dynamic Response of a Ring-Supported Cylinder to Time-Dependent Loads", Jour. Spacecraft and Rockets, vol. 3, pp. 1369-1376 (1966).

39. Hu, W.C.L., J.F. Gormley, and U.S. Lindholm, "An Analytical and Experimental Study of Vibrations of Ring-Stiffened Cylindrical Shells", Technical Report No. 9, Southwest Research Institute, San Antonio, Texas (June 1967).

40. McGrattan, R.J. and E.L. North, "Vibration Analysis of Shells Using Discrete Mass Techniques", Jour. Engr. Indust., Trans. ASME, vol. 89, pp. 766-772 (Nov. 1967).

41. Hung, F.C., et. al., "Dynamics of Shell-Like Lifting Bodies Part I. The Analytical Investigation", Technical Report AFFDL-TR-65-17, Part I, Wright-Patterson AFB, Ohio (June 1965).

42. Park, A.C., et. al., "Dynamics of Shell-Like Lifting Bodies Part II. The Experimental Investigation", Technical Report AFFDL-TR-65-17, Part II, Wright-Patterson AFB, Ohio (June 1965).

43. Wah, T., "Vibration of Cylindrical Gridwork Shells", AIAA Jour., vol. 3, pp. 1467-1475 (1965).

44. Berglund, J.W. and J.M. Klosner, "Interaction of a Ring-Reinforced Shell and a Fluid Medium", Jour. Appl. Mech., vol. 35, pp. 139-147 (1968).

45. Scruggs, R.M., C.V. Pierce and J.R. Reese, "An Analytical and Experimental Study of the Vibration of Orthogonally Stiffened Cylindrical Shells", AIAA Paper 68-349, AIAA/ASME 9th Structures, Structural Dynamics and Materials Conference, Palm Springs, Calif. (April 1968).

46. Egle, D.M. and J.L. Sewall, "An Analysis of Free Vibration of Orthogonally Stiffened Cylindrical Shells with Stiffeners Treated as Discrete Elements", AIAA Jour., vol. 6, pp. 518-526 (March 1968).

47. Soder, K.E., Jr., "An Analysis of Free Vibration of Thin Cylindrical Shells with Rings and Stringers Treated as Discrete Elements Which May Be Nonsymmetric, Eccentric, and Arbitrarily Spaced", Ph.D. Dissertation, School of Aerospace and Mechanical Engineering, University of Oklahoma, Norman, Okla. (1968).

48. Flugge, W., "Stresses in Shells", Springer-Verlag, Berlin, (1962).

49. Meirovitch, L., "Analytical Methods in Vibration", MacMillan Co., New York, pp. 225-233 (1967).

50. Card, M.F. and R.M. Jones, "Experimental and Theoretical Results for Buckling of Eccentrically Stiffened Cylinders", NASA TN D-3639 (1966).

51. Forsberg, K., "Influence of Boundary Conditions on the Modal Characteristics of Thin Cylindrical Shells", AIAA Journal, Vol. 2, No. 12, pp. 2150-2157 (1964).

52. Huffington, N.J., Jr., "Bending Athwart a Parallel-Stiffened Plate", Jour. Appl. Mech., Vol. 34, No. 2, pp. 278-282 (1967).

53. Wilkinson, J.H., "The Algebraic Eigenvalue Problem", Claredon Press-Oxford (1965).

APPENDIX I

In this appendix, an approximate method for calculating the cross-stiffening energy of the discrete rings and stiffeners is developed. If the stiffener is not attached at a single line, as in the case of the integral stiffener shown in Figure (AI-1), both the flexural and extensional stiffness of the shell, perpendicular to the stiffener axis, will be increased. This increase is a local effect and should be treated as such in an analysis of discrete stiffeners.

Huffington (52) detailed an approximate technique for including the flexural cross stiffening in a smeared stiffener analysis. The following analysis is based in part on Huffington's work and will consider only flexural cross-stiffening. It is assumed that, for the purpose of determining the cross-stiffening energy, the shell-stiffener is in a state of pure bending and the shell and stiffener are of the same material.

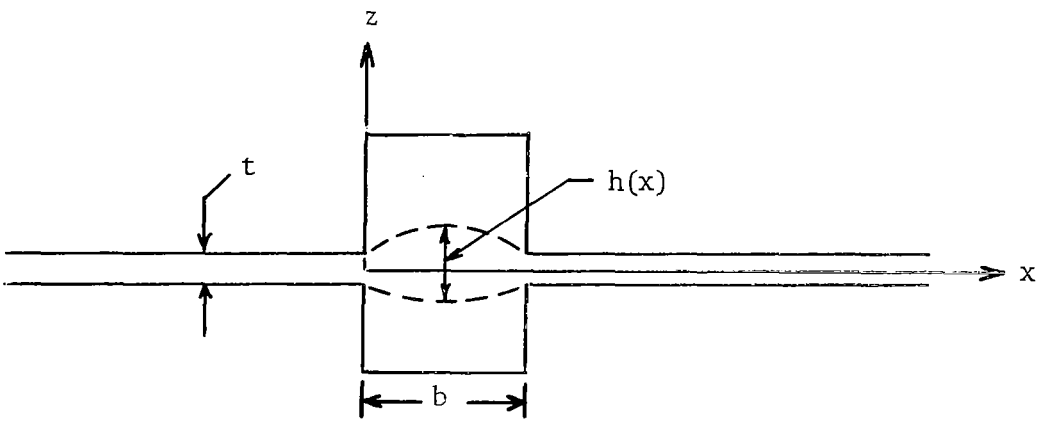

FIGURE AI-1. Geometry of Integral Ring-Shell Combination.

Consider the integral ring stiffener shown in Figure (AI-1). Following Huffington, the ring-shell combination is replaced by a non-uniform shell of thickness, h(x), whose resistance to bending is equivalent to the actual ring and shell. The flexural strain energy of this non-uniform section is

$$V = 1/2 \int_0^{2\pi} \int_0^b \{D_x\, w,_{xx}^2 + \nu\, (D_x + D_y)\, w,_{xx}\, w,_{yy} + D_y\, w,_{yy}^2\}\; dx\, R d\theta \tag{AI-1}$$

The two terms with the coefficient D_y in this equation represent the energy due to stiffening along the ring axis. The two remaining terms are the cross-stiffening energies, and if pure bending perpendicular to the stiffener axis is assumed ($w,_{yy} = -\nu\, w,_{xx}$), equation (AI-1) may be written as

$$V_{cs} = \frac{1-\nu^2}{2} \int_0^{2\pi} \int_0^b D_x\, w,_{xx}^2\, dx\, R d\theta \tag{AI-2}$$

Both D_x and $w,_{xx}$ are functions of x in the interval $0 \leq x \leq b$. It is assumed that the integral

$$\int_0^b D_x\, w,_{xx}^2\, dx = b\, \overline{D}_x\, \bar{w},_{xx}^2 \tag{AI-3}$$

where $\overline{D}_x$ is an equivalent flexural rigidity, calculated to yield the correct strain energy for the pure bending case, and can be shown to be

$$\overline{D}_x = \frac{E\, b}{12(1-\nu^2) \int_0^b \frac{dx}{h^3(x)}} \tag{AI-4}$$

and $\bar{w},_{xx}$ is taken equal to the curvature of the shell at the line of attachment of the ring to the shell.

Equation (AI-2) is the flexural energy of the ring and shell combined. The energy of the shell has been included in equation (7) and should be subtracted from the cross stiffening energy. Thus, the energy due to flexural cross-stiffening of the ring is

$$V_{csr} = 1/2\ E_r\ I_{csr} \int_o^{2\pi} [w,_{xx}^2]_{x=x_k} R d\theta \tag{AI-5}$$

where

$$I_{csr} = \frac{b}{12}\left[\frac{b}{\int_o^b \frac{dx}{h^3(x)}} - t^3 \right] \tag{AI-6}$$

In a similar manner, the cross-stiffening energy of a stringer may be shown to be

$$V_{css} = 1/2\ E_s\ I_{css} \int_o^a (1/R^4)\ [w,_{\theta\theta}^2]_{\theta=\theta_\ell} dx \tag{AI-7}$$

where

$$I_{css} = \frac{c}{12}\left[\frac{c}{\int_o^c \frac{dy}{h^3(y)}} - t^3 \right] \tag{AI-8}$$

In equation (AI-8) c is the width of the stringer at the shell-stringer junction and y is the circumferential distance ($R\theta$).

APPENDIX II

Matrix Elements in Rayleigh-Ritz Vibration Analysis

This appendix contains detailed expressions for the unprimed coefficients in equations (37a-f) and the matrix elements of equation (38). The primed coefficients, A'_{ijmn}, B'_{ijmn}, etc., may be calculated by interchanging sin ( ) and cos ( ) and be replacing $\bar{y}_{s\ell}$ with $-\bar{y}_{s\ell}$ and $I_{yzs\ell}$ with $-I_{yzs\ell}$ in the expressions for the unprimed coefficients. For example,

$$NN'_{ijmn} = \delta_{jn} \sum_{k=1}^{K} M_{rk}\bar{x}_{rk} \; V_m U_i \;_{x_k}$$

$$+ I_{V'_m U_i} \sum_{\ell=1}^{L} M_{s\ell}\bar{y}_{s\ell} \; (\cos n\theta_\ell \sin j\theta_\ell)$$

The terms that are bracketed and subscripted x_k, as an example $[U_m U_i]_{x_k}$, indicate that the expression is evaluated at the location x_k. The terms like $I_{U_m U_i}$, $I_{V'_m V_i}$ etc., are a short notation for an integral; for example

$$I_{U_m U_i} = \frac{1}{a} \int_o^a U_m(x) U_i(x)\, dx$$

$$I_{V'_m V'_i} = \frac{1}{a} \int_o^a V'_m(x) V'_i(x)\, dx$$

The following definitions have been used to shorten the expressions for the coefficients:

$$M_{s\ell} = \frac{\rho_{s\ell} A_{s\ell}}{\rho_c \pi R t}$$

$$M_{rk} = \frac{\rho_{rk} A_{rk}}{\rho_c a t}$$

$$S_{s\ell} = \frac{(1-\nu^2) E_{s\ell} A_{s\ell}}{E_c \pi R t}$$

$$S_{rk} = \frac{(1-\nu^2) E_{rk} A_{rk}}{E_c a t}$$

$$T_{s\ell} = \frac{(1-\nu^2)(GJ)_{s\ell}}{E_c \pi R^3 t}$$

$$T_{rk} = \frac{(1-\nu^2)(GJ)_{rk}}{E_c a R^2 t}$$

The term δ_{jn} is the Kronecker delta and is equal to zero except for j=n.

The unprimed coefficients are as follows:

$$A_{ijmn} = \delta_{jn} \left[R^2 I_{U_m' U_i'} + \left(\frac{1-\nu}{2}\right) \frac{TRj^2}{t} I_{U_m U_i} + \frac{j^4}{R^2} \sum_{k=1}^{K} \frac{S_{rk} I_{zzrk}}{A_{rk}} \left[U_m U_i\right]_{x_k} \right]$$

$$+ R^2 I_{U_m' U_i'} \sum_{\ell=1}^{L} S_{s\ell} (\cos n\theta_\ell \cos j\theta_\ell)$$

$$B_{ijmn} = \delta_{jn} \left[j^2 I_{V_m V_i} + \left(\frac{1-\nu}{2}\right)\left(R^2 + \frac{t^2}{4}\right) I_{V_m' V_i'} + j^2 \sum_{k=1}^{K} S_{rk} \left[V_m V_i\right]_{x_k} \right]$$

$$+ R^2 I_{V_m'' V_i''} \sum_{\ell=1}^{L} \frac{S_{s\ell} I_{zzs\ell}}{A_{s\ell}} (\sin \theta_\ell \sin j\theta_\ell)$$

$$C_{ijmn} = \delta_{jn} \left[\left[\frac{TR}{t} + \left(\frac{TR-t}{t}\right)(j^4 - 2_j{}^2)\right] I_{W_m W_i} + \frac{t^2 R^2}{12} I_{W_m'' W_i''} \right.$$

$$- \frac{t^2 \nu j^2}{12} (I_{W_m''} I_{W_i} + I_{W_m W_i''}) + (\frac{1-\nu}{2})(\frac{R^3 T}{t} - R^2 + \frac{t^2}{4}) j^2 I_{W_m' W_i'}$$

$$+ \sum_{k=1}^{K} \Bigg[S_{rk} \Bigg\{ \left(\frac{I_{xxrk} j^4}{R^2 A_{rk}} + \frac{2\bar{z}_{rk} j^2}{R} + 1 \right) [W_m W_i]_{x_k}$$

$$+ \left(\bar{x}_{rk} + n^2 \frac{I_{xzrk}}{R A_{rk}} \right) [W_m W_i' + W_m' W_i]_{x_k} + \frac{I_{zzrk}}{A_{rk}} [W_m' W_i']_{x_k} \Bigg\}$$

$$+ T_{rk} R^2 j^2 [W_m' W_i']_{x_k} + \frac{R^2 I_{csrk}}{A_{rk}} [W_m'' W_i'']_{x_k} \Bigg] \Bigg]$$

$$+ R^2 \sum_{\ell=1}^{L} \Bigg[\frac{S_{s\ell}}{A_{s\ell}} \left(I_{yys\ell} I_{W_m'' W_i''} + \frac{n^2 j^2}{R^4} I_{css\ell} I_{W_m W_i} \right)$$

$$(\cos n\theta_\ell \cos j\theta_\ell) + jnT_{s\ell} I_{W_m' W_i'} (\sin n\theta_\ell \sin j\theta_\ell) \Bigg]$$

$$D_{ijmn} = \delta_{jn} jR \left\{ \nu I_{V_m U_i'} - (\frac{1-\nu}{2}) I_{V_m' U_i} + \frac{j^3}{R} \sum_{k=1}^{K} S_{rk} \bar{x}_{rk} [V_m U_i]_{x_k} \right\}$$

$$- R^2 I_{V_m' U_i'} \sum_{\ell=1}^{L} S_{s\ell} \bar{y}_{s\ell} (\sin n\theta_\ell \cos j\theta_\ell)$$

$$E_{ijmn} = \delta_{jn} \Bigg\{ \nu R I_{W_m U_i'} - \frac{t^2 R}{12} I_{W_m' U_i'} + (\frac{1-\nu}{2}) \frac{(RT-t)Rj^2}{t} I_{W_m' U_i}$$

$$+ j^2 \sum_{k=1}^{K} S_{rk} \Bigg[\left(\frac{x_{rk}}{R} + j^2 \frac{I_{xzrk}}{R^2 A_{rk}} \right) [W_m U_i]_{x_k}$$

$$+ \frac{I_{zzrk}}{A_{rk}R} [W_m'U_i]_{x_k} \Bigg] \Bigg\} - R^2 I_{W_m''U_i'} \sum_{\ell=1}^{L} S_{s\ell} \bar{z}_{s\ell} (\cos n\theta_\ell \cos j\theta_\ell)$$

$$F_{ijmn} = \delta_{jn} j \Bigg\{ I_{W_m V_i} - \frac{t^2 \nu}{12} I_{W_m'' V_i} + \left(\frac{1-\nu}{2}\right) \frac{t^2}{4} I_{W_m' V_i'}$$

$$+ \sum_{k=1}^{K} S_{rk} \left[\left(1 + \frac{j^2 \bar{Z}_{rk}}{R}\right) [W_m V_i]_{x_k} + \bar{X}_{rk} [W_m' V_i]_{x_k} \right] \Bigg\}$$

$$+ R^2 I_{W_m'' V_i''} \sum_{\ell=1}^{L} \frac{S_{s\ell} I_{yzs\ell}}{A_{s\ell}} (\cos n\theta_\ell \sin j\theta_\ell)$$

$$G_{ijmn} = R^2 I_{U_m' U_i'} \sum_{\ell=1}^{L} S_{s\ell} (\sin n\theta_\ell \cos j\theta_\ell)$$

$$H_{ijmn} = -R^2 I_{W_m'' U_i'} \sum_{\ell=1}^{L} S_{s\ell} \bar{z}_{s\ell} (\sin n\theta_\ell \cos j\theta_\ell)$$

$$M_{ijmn} = R^2 \sum_{\ell=1}^{L} \Bigg\{ \frac{S_{s\ell}}{A_{s\ell}} \left[I_{yys\ell} I_{W_m'' W_i''} + \frac{n^2 j^2}{R^4} I_{css\ell} I_{W_m W_i} \right]$$

$$(\sin n\theta_\ell \cos j\theta_\ell) - T_{s\ell} jn (\cos n\theta_\ell \sin j\theta_\ell) I_{W_m' W_i'} \Bigg\}$$

$$DD_{ijmn} = R^2 I_{W_m'' V_i''} \sum_{\ell=1}^{L} \frac{S_{s\ell} I_{yzs\ell}}{A_{s\ell}} (\sin n\theta_\ell \sin j\theta_\ell)$$

$$EE_{ijmn} = -R^2 I_{V_m' V_i''} \sum_{\ell=1}^{L} \frac{S_{s\ell} I_{zzs\ell}}{A_{s\ell}} (\cos n\theta_\ell \sin j\theta_\ell)$$

$$FF_{ijmn} = -R^2 I_{U_m' V_i''} \sum_{\ell=1}^{L} S_{s\ell} \bar{y}_{s\ell} (\sin n\theta_\ell \sin j\theta_\ell)$$

$$GG_{ijmn} = R^2 I_{V'_m U'_i} \sum_{\ell=1}^{L} S_{s\ell} \bar{y}_{s\ell} (\cos n\theta_\ell \cos j\theta_\ell)$$

$$HH_{ijmn} = - R^2 I_{U'_m W'_i} \sum_{\ell=1}^{L} S_{s\ell} \bar{z}_{s\ell} (\sin n\theta_\ell \cos j\theta_\ell)$$

$$MM_{ijmn} = -R^2 I_{V'_m W'_i} \sum_{\ell=1}^{L} \frac{S_{s\ell} I_{yzs\ell}}{A_{s\ell}} (\cos n\theta_\ell \cos j\theta_\ell)$$

$$N_{ijmn} = \delta_{jn} \left\{ I_{U_m U_i} + \sum_{k=1}^{K} M_{rk} \left(1 + \frac{j^2}{R^2} \frac{I_{zzrk}}{A_{rk}}\right) [U_m U_i]_{x_k} \right\}$$

$$+ I_{U_m U_i} \sum_{\ell=1}^{L} M_{s\ell} (\cos n\theta_\ell \cos j\theta_\ell)$$

$$P_{ijmn} = -\delta_{jn} \sum_{k=1}^{K} M_{rk} \left\{ \bar{z}_{rk} [W'_m U_i]_{x_k} - \frac{j^2}{R^2} \frac{I_{xzrk}}{A_{rk}} [W_m U_i]_{x_k} \right\}$$

$$- I_{W'_m U_i} \sum_{\ell=1}^{L} M_{s\ell} \bar{z}_{s\ell} (\cos n\theta_\ell \cos j\theta_\ell)$$

$$Q_{ijmn} = \delta_{jn} \left\{ I_{V_m V_i} + \sum_{k=1}^{K} M_{rk} [V_m V_i]_{x_k} \right\}$$

$$+ \sum_{\ell=1}^{L} M_{s\ell} \left(\frac{I_{zzs\ell}}{A_{s\ell}} I_{V'_m V'_i} + I_{V_m V_i}\right) (\sin n\theta_\ell \sin j\theta_\ell)$$

$$R_{ijmn} = \frac{\delta_{jn} j}{R} \sum_{k=1}^{K} M_{rk} \bar{z}_{rk} [W_m V_i]_{x_k} + \sum_{\ell=1}^{L} M_{s\ell} \left\{ \frac{I_{yzs\ell}}{A_{s\ell}} I_{W'_m V'_i} \right.$$

$$\left. (\cos n\theta_\ell \sin j\theta_\ell) + \frac{n}{R} \bar{z}_{s\ell} I_{W_m V_i} (\sin n\theta_\ell \sin j\theta_\ell) \right\}$$

$$S_{ijmn} = \delta_{jn} \left\{ I_{W_m W_i} + \sum_{k=1}^{K} M_{rk} \left[\left(1 + \frac{I_{xxrk} j^2}{A_{rk} R^2}\right) [W_m W_i]_{x_k} \right.\right.$$

$$\left.\left. + \bar{x}_{rk} \left([W_m W_i']_{x_k} + [W_m' W_i]_{x_k}\right) + \left(\frac{I_{xxrk} + I_{zzrk}}{A_{rk}}\right) [W_m' W_i']_{x_k} \right]\right\}$$

$$+ \sum_{\ell=1}^{L} M_{s\ell} \left\{ \left[I_{W_m W_i} + \frac{I_{yys\ell}}{A_{s\ell}} I_{W_m' W_i'}\right] (\cos n\theta_\ell \cos j\theta_\ell) \right.$$

$$+ I_{W_m W_i} \left[\frac{jn}{R^2} \left(\frac{I_{yys\ell} + I_{zzs\ell}}{A_{s\ell}} \right) (\sin n\theta_\ell \sin j\theta_\ell) \right.$$

$$\left.\left. - \frac{\bar{y}_{s\ell} j}{R} (\cos n\theta_\ell \sin j\theta_\ell) - \frac{\bar{y}_{s\ell} n}{R} (\sin n\theta_\ell \cos j\theta_\ell) \right]\right\}$$

$$T_{ijmn} = I_{U_m U_i} \sum_{\ell=1}^{L} M_{s\ell} (\sin n\theta_\ell \cos j\theta_\ell)$$

$$U_{ijmn} = - I_{W_m' U_i} \sum_{\ell=1}^{L} M_{s\ell} \bar{z}_{s\ell} (\sin n\theta_\ell \cos j\theta_\ell)$$

$$V_{ijmn} = - \sum_{\ell=1}^{L} M_{s\ell} \left[I_{V_m V_i} + \frac{I_{zzs\ell}}{A_{s\ell}} I_{V_m' V_i'}\right] (\cos n\theta_\ell \sin j\theta_\ell)$$

$$W_{ijmn} = \sum_{\ell=1}^{L} M_{s\ell} \left[\frac{I_{yzs\ell}}{A_{s\ell}} I_{W_m' V_i'} (\sin n\theta_\ell \sin j\theta_\ell) \right.$$

$$\left. - \frac{n}{R} \bar{z}_{s\ell} I_{W_m V_i} (\cos n\theta_\ell \sin j\theta_\ell) \right]$$

$$X_{ijmn} = - \sum_{\ell=1}^{L} M_{s\ell} \left[\bar{z}_{s\ell} \frac{j}{R} I_{V_m W_i} (\cos n\theta_\ell \sin j\theta_\ell) \right.$$

$$+ \frac{I_{yzs\ell}}{A_s} (\cos n\theta_\ell \cos j\theta_\ell)\ I_{V_m'W_i'}\Big]$$

$$Y_{ijmn} = \sum_{\ell=1}^{L} M_{s\ell} \Bigg\{ \Big[I_{W_mW_i} + \frac{I_{yys\ell}}{A_{s\ell}} I_{W_m'W_i'}\Big] (\sin n\theta_\ell \cos j\theta_\ell)$$

$$- I_{W_mW_i} \Bigg[\frac{jn}{R^2} \Big(\frac{I_{yys\ell} + I_{zzs\ell}}{A_{s\ell}}\Big)(\cos n\theta_\ell \sin j\theta_\ell)$$

$$- \frac{\bar{y}_{s\ell} n}{R} (\cos n\theta_\ell \cos j\theta_\ell) + \frac{\bar{y}_{s\ell} j}{R} (\sin n\theta_\ell \sin j\theta_\ell)\Bigg]\Bigg\}$$

$$NN_{ijmn} = \frac{j\delta_{jn}}{R} \sum_{k=1}^{K} M_{rk}\bar{x}_{rk} [V_mU_i]_{x_k} - I_{V_m'U_i} \sum_{\ell=1}^{L} M_{s\ell}\ \bar{y}_{s\ell}$$

$$(\sin n\theta_\ell \cos j\theta_\ell)$$

$$RR_{ijmn} = -I_{U_mV_i'} \sum_{\ell=1}^{L} M_{s\ell}\ \bar{y}_{s\ell}\ (\sin n\theta_\ell \sin j\theta_\ell)$$

$$TT_{ijmn} = I_{V_m'U_i} \sum_{\ell=1}^{L} M_{s\ell}\ \bar{y}_{s\ell}\ (\cos n\theta_\ell \cos j\theta_\ell)$$

$$UU_{ijmn} = - I_{U_mW_i'} \sum_{\ell=1}^{L} M_{s\ell}\ \bar{z}_{s\ell}\ (\sin n\theta_\ell \cos j\theta_\ell)$$

APPENDIX III

The initial calculations of the eigenvalues and eigenvectors of equation (41) were carried out with digital computer subroutines supplied by NASA Langley Research Center. Because of the relatively large size of the eigenvalue problem, the subroutines (EIGEN and JACOBI) required 30 minutes or more for the solution of a typical (57 X 57) size problem. This does not include generation of the mass and stiffness matrices (10 minutes) or compile time (10 minutes). It was felt that this excessive time warranted a brief study of the techniques available for the solution of eigenvalue problems with the objective of decreasing the time needed for the calculations.

The first step in solving the linear symmetric eigenvalue problem

$$[K]\ \{x\} = \omega^2\ [M]\ \{x\} \qquad \text{(AIII-1)}$$

is to transform it to the standard form

$$[A]\ \{x\} = \lambda\ \{x\} \qquad \text{(AIII-2)}$$

Two methods for accomplishing this were considered the first (called transformation 1) involves finding the eigenvalues and eigenvectors of [M] by solving

$$[M]\ \{u\} = \Delta\ \{u\} \qquad \text{(AIII-3)}$$

thus allowing [M] to be expressed as

$$[M] = [U]\ [\ulcorner D \lrcorner]\ [U]^T \qquad \text{(AIII-4)}$$

where the columns of [U] are the eigenvectors of (AIII-3) and $[\ulcorner D \lrcorner]$ is a diagonal matrix of the eigenvalues of [M]. It has been assumed that the eigenvectors have been normalized such that

$$[U]^T[U] = 1$$

If [M] is positive definite, $[\lceil D \rfloor]$ may be written as

$$[\lceil D \rfloor] = [\lceil D' \rfloor]\ [\lceil D' \rfloor] \qquad \text{(AIII-5)}$$

where the elements of $[\lceil D' \rfloor]$ are the positive square roots of the corresponding elements in $[\lceil D \rfloor]$. Using equations (AIII-4,5), equation (AIII-1) may be transformed into

$$[A]\ \{v\} = \omega^2\ \{v\} \qquad \text{(AIII-6)}$$

where $[A] = [\lceil D' \rfloor]^{-1}\ [U]^T [K]\ [U]\ [\lceil D' \rfloor]^{-1}$

$$\{v\} = [\lceil D' \rfloor]\ [U]^T\ \{x\} \qquad \text{(AIII-7)}$$

The eigenvalues of (AIII-6) are the eigenvalues of (AIII-1) and the eigenvectors of (AIII-1) may be determined from the eigenvectors of (AIII-6) and equation (AIII-7).

Note that to solve equation (AIII-1) with this transformation, it is necessary to do two eigenvalue calculations and the accuracy of the result is dependent on the accuracy to which the eigenvectors of [M] are calculated.

Another method (transformation 2) of transforming equation (AIII-1) into the standard form utilizes triangular matrices. If the matrix [M] can be expressed as

$$[M] = [L]\ [L]^T \qquad \text{(AIII-8)}$$

where [L] is a lower triangular matrix,

then (AIII-1) may be transformed into (AIII-6) with

$$[A] = [L]^{-1}\ [K]\ ([L]^{-1})^T$$

and

$$\{v\} = [L]^T\ \{x\} \qquad \text{(AIII-9)}$$

Calculation of [L] and $[L]^{-1}$ is relatively simple. It may be shown that

$$\ell_{ij} = \begin{cases} \left[m_{ij} - \sum_{n=1}^{j-1} \ell_{in}\, \ell_{jn}\right]^{1/2} & i=j \\ \left[m_{ij} - \sum_{n=1}^{j-1} \ell_{in}\, \ell_{jn}\right] / \ell_{jj} & i>j \\ 0 & i<j \end{cases}$$

and

$$\ell_{ij}^{-1} = \begin{cases} 0 & i<j \\ 1/\ell_{ii} & i=j \\ \left[\sum_{k=j}^{i-1} - \ell_{ik}\, \ell_{kj}^{-1}\right] / \ell_{ii} & i>j \end{cases}$$

where ℓ_{ij} and ℓ_{ij}^{-1} are the elements of [L] and $[L]^{-1}$, respectively.

The advantage of transformation 2 over transformation 1 lies in not having to calculate the eigenvalues and eigenvectors of [M], which is the most time consuming step of transformation 1.

It should be noted that both of these transformations may be used to reduce (AIII-1) to

$$[A]\ \{q\} = \frac{1}{\omega^2}\ \{q\} \qquad \text{(AIII-10)}$$

by simply interchanging [K] and [M] in the transformation. This form is not obtainable if rigid body modes (ω=0) are possible solutions to the problem. It is desirable because the eigenvalue subroutines considered here calculated the largest eigenvalue with the highest degree of accuracy. Thus, if the problem is in the form (AIII-10) this corresponds to the lowest natural frequency.

Two techniques for solving the standard eigenvalue problem were considered. The Householder-Givens method, which is reported to be a

very fast technique, worked very well for problems of size (10 X 10) but failed for a large matrix (60 X 60) and was abandoned. The other method is the well-known Jacobi method, an iteration technique which reduces the matrix [A], equation (AIII-2) to a diagonal matrix by a series of plane rotations, each one of which reduces one of the off-diagonal elements in the matrix to zero. In each step, the largest off diagonal element is annihilated and the process is repeated until the largest off diagonal element is less that the product of the smallest eigenvalue and a preassigned small number (called an indicator). The value of the indicator determines the accuracy of the eigenvalues and eigenvectors.

Several variations of transformation 2 and the Jacobi method were used to calculate the eigenvalues and eigenvectors of a (60 X 60) problem of the type generated by the analysis described in this report. The results were compared to those of the subroutines EIGEN and JACOBI (which uses transformation 1 and the Jacobi method with an indicator of $.75 \times 10^{-8}$), which required 34 minutes to do the calculation. The combination which was fastest while still maintaining acceptable accuracy was transformation 2, form (AIII-10) and an indicator of 0.75×10^{-1}. The time for this calculation was 11 minutes and the lowest frequency was correct to 8 significant figures, the highest frequency was correct to 2 significant figures, the eigenvectors of the lowest frequency were correct to 4 significant figures in the largest components. The eigenvectors of the highest frequencies were not correct. Decreasing the indicator increased the computation time and the accuracy. For an indicator of 0.75×10^{-2}, the computation time was 15 minutes and the accuracies were as follows.

	Number of correct significant figures
Lowest frequency	8
Highest frequency	3
Predominant terms in eigenvector of lowest frequency	6
Smaller terms in eigenvectors of lowest frequency	2
Predominant terms in eigenvectors of highest frequency	2
Smaller terms in eigenvectors of highest frequency	-

It was concluded that using transformation 2 to reduce the original equation to the form (AIII-10) and the Jacobi method with an indicator of 0.75×10^{-2} was sufficiently accurate and reduced the computation time by a factor of 2 compared to using transformation 1, the Jacobi method and an indicator of 0.75×10^{-8}.

It should be noted that the results presented in the body of this report were calculated with double precision versions of two IBM supplied subroutines (EIGEN and NROOT) which utilize transformation 1, the Jacobi method, and an indicator of 10^{-6}.

Further details on the two transformations described here are given in reference (53). In that reference, the decomposition (AIII-8) is called the Cholesky decomposition.

NASA-Langley, 1969 —— 32 CR-1316